THE ASTROPHYSICAL JOURNAL, 429:781–796, 1994 July 10

MAGNETOCENTRIFUGALLY DRIVEN FLOWS FROM YOUNG STARS AND DISKS. I. A GENERALIZED MODEL

FRANK SHU, JOAN NAJITA, EVE OSTRIKER, AND FRANK WILKIN
Astronomy Department, University of California, Berkeley, CA 94720
STEVEN RUDEN
Department of Physics, University of California, Irvine, CA 92717
AND
SUSANA LIZANO
Instituto de Astronomia, Universidad Nacional Autonoma de Mexico, Apdo. Postal 70-264, DF 04510 Mexico City, Mexico
Received 1993 September 9; accepted 1994 January 11

ABSTRACT

We propose a generalized model for stellar spin-down, disk accretion, and truncation, and the origin of winds, jets, and bipolar outflows from young stellar objects. We consider the steady state dynamics of accretion of matter from a viscous and imperfectly conducting disk onto a young star with a strong magnetic field. For an aligned stellar magnetosphere, shielding currents in the surface layers of the disk prevent stellar field lines from penetrating the disk everywhere except for a range of radii about $\varpi = R_x$, where the Keplerian angular speed of rotation Ω_x equals the angular speed of the star Ω_*. For the low disk accretion rates and high magnetic fields associated with typical T Tauri stars, R_x exceeds the radius of the star R_* by a factor of a few, and the inner disk is effectively truncated at a radius R_t somewhat smaller than R_x. Where the closed field lines between R_t and R_x bow sufficiently inward, the accreting gas attaches itself to the field and is funneled dynamically down the effective potential (gravitational plus centrifugal) onto the star. Contrary to common belief, the accompanying magnetic torques associated with this accreting gas may transfer angular momentum mostly to the disk rather than to the star. Thus, the star can spin slowly as long as R_x remains significantly greater than R_*. Exterior to R_x field lines threading the disk bow outward, which makes the gas off the midplane rotate at super-Keplerian velocities. This combination drives a magnetocentrifugal wind with a mass-loss rate $\dot{M}_w$ equal to a definite fraction f of the disk accretion rate $\dot{M}_D$. For high disk accretion rates, R_x is forced down to the stellar surface, the star is spun to breakup, and the wind is generated in a manner identical to that proposed by Shu, Lizano, Ruden, & Najita in a previous communication to this journal. In two companion papers (II and III), we develop a detailed but idealized theory of the magnetocentrifugal acceleration process.

Subject headings: accretion, accretion disks — MHD — stars: formation — stars: magnetic fields — stars: mass loss — stars: pre–main sequence — stars: rotation

1. INTRODUCTION

1.1. *Motivation for Present Study*

Bipolar molecular outflows and the related phenomena of optical jets and T Tauri winds remain among the most intriguing and important observational discoveries in the field of star formation (see, e.g., the reviews of Lada 1985; Mundt 1985; Snell 1987; Fukui 1989; Reipurth 1990; Edwards et al. 1993a). Although astronomers have made considerable progress toward understanding the flow morphology, jet propagation, shock diagnostics, and wind chemistry; they have reached no consensus concerning the basic driving mechanism for these outflows (see, e.g., Königl & Ruden 1993).

Theoretical ideas for the ultimate source of the momentum in the outflows include winds from the central protostars (e.g., Draine 1983) or from their circumstellar disks (e.g., Lovelace 1976; Uchida & Shibata 1985). Flows driven by Alfvén waves may suffice to explain the energetics of the T Tauri winds with mass-loss rates $\dot{M}_w \lesssim 10^{-8}\ M_\odot\ \mathrm{yr}^{-1}$ (DeCampli 1981; Holzer et al. 1983; Lago 1984), but the mass-loss rates $\dot{M}_w \gtrsim 10^{-6}\ M_\odot\ \mathrm{yr}^{-1}$ associated with the deeply embedded sources that drive most bipolar molecular flows probably require both strong magnetic fields and rapid rotation—for example, a magnetized protostar rotating near break-up (Hartmann & MacGregor 1982, hereafter HM), or a centrifugally supported disk with substantial poloidal magnetic fields of an open geometry (Blandford & Payne 1982; Pudritz & Norman 1983, 1986; Königl 1989), or a combination of a strongly magnetized star plus an adjoining Keplerian disk (Shu et al. 1988, hereafter SLRN).

1.2. *Pure Disk Winds*

Magnetocentrifugal models of pure disk winds have been worked out in some detail. For bipolar flinging to occur, the magnetic lines of force must bend over from the vertical by more than 30° after the sonic (or in a different representation, the slow MHD) transition has been made at the top and bottom surfaces of the disk (in the limit of a cold flow). To accomplish this task in models of disks around low-mass young stellar objects (YSOs), Wardle & Königl (1993) invoke inward slip speeds v_d of neutral gas relative to the ions and field (ambipolar diffusion) between ~ 0.1 and 1 times the sonic value in the midplane of the disk. Since the inward pinching of the poloidal field is greatest in the midplane, the field lines at higher latitudes lag radially and bow outward. Magnetocentrifugal effects along the connected field line (associated with the terms $B_\varpi B_\varphi/4\pi$ and $B_z B_\varphi/4\pi$ in Maxwell's stress tensor expressed in cylindrical coordinates ϖ, φ, z centered on the star) then launch the gas near the surface of the disk into a wind.

While mechanistically attractive, the pure-disk wind applied to YSOs has problems meeting the astronomical constraints. (1) The large radial drift needed in the midplane (enforced by rotation at sub-Keplerian speeds) at $\varpi \sim 100$ AU (where observed disks are believed to end and cannot be replenished by inflow from yet larger radii if infall from the parent cloud core has ceased) leads to accretion timescales ϖ/v_d about three orders of magnitude shorter than the values, 10^6–10^7 yr, inferred for T Tauri disks on empirical grounds (e.g., Strom et al. 1989; Beckwith et al. 1990). (2) Equilibrium calculations by Umebayashi & Nakano (1988) for minimum-mass models of the solar nebula show, in fact, very *low* ionization levels in the midplane at all but the innermost disk radii. Surface densities much in excess of $\sim 10^2$ g cm^{-2} effectively shut off all sources of external ionization, whereas high volume densities lead to rapid recombinations against internal sources of ionization such as natural radioactivity. Thus, ohmic dissipation and ambipolar diffusion would quickly rid the disk interior of magnetic fields with strengths and curls (curvatures across the midplane) as large as those required in the disk-wind models for all ϖ between ~ 0.1 and 20 AU. The surface layers of the disk are still electrically conducting, but it remains to be seen if they could support magnetic fields with the requisite geometry and strength.

At small ϖ, heating by stellar photons and viscous accretion will provide a relatively abundant source of electrons and ions through the thermal ionization of metals. Thus, good mechanical coupling of the gas to preexisting magnetic fields in the disk will exist only within several stellar radii of the central star. In addition, direct observational evidence suggests that strong YSO winds correlate with the presence of inner disks (Cabrit et al. 1990). The deduced importance of the inner disk is also consistent with the empirical discovery of fast, lightly ionized winds from YSOs (Bally & Stark 1983; Lizano et al. 1988; Koo 1989; Masson et al. 1990; Bachiller & Cernicharo 1990; Giovanardi et al. 1992; Ruiz et al. 1992; Russell et al. 1992; Carlstrom et al. 1994). The speeds of such winds—combined with the observation that in two outflow sources of moderate luminosity, HH 7-11 and L1551, the fast winds contain both H I and CO—suggest that the driving flows must originate from $\varpi \lesssim$ several stellar radii, where the depth of the gravitational potential leads to characteristic speeds of ~ 200 km s^{-1} and where the temperatures are high enough to dissociate molecular hydrogen but not carbon monoxide (see Glassgold et al. 1989, 1991; Ruden et al. 1990).

1.3. *Pure Stellar Winds*

The idea that rapid rotating magnetized stars might suffer enhanced mass loss goes back at least to the early papers of Mestel and his colleagues (e.g., Mestel 1968). HM made the first concrete application to the phenomenon of bipolar molecular outflows. Unfortunately, because they used the formalism of Weber & Davis (1967), they could only follow the part of the flow in the equatorial plane that occurs in directions orthogonal to those indicated by the observations. Moreover, because they attempted to explain molecular outflows with observed velocities of ~ 10–100 km s^{-1} as a direct manifestation of protostellar winds, they adopted characteristic radii ($\sim 10^{14}$ cm), effective temperatures (~ 500–1500 K), and surface magnetic fields (~ 1–10 G) for their quasi-static protostars that differ considerably from the values allowed by both contemporary observations and theory. Nevertheless, provided they had the freedom to adjust the density of the gas at the sonic transition, HM discovered the important point that magnetized stars rotating near breakup could shed mass and angular momentum at enormous rates from their equatorial regions.

SLRN modified the model of HM by (1) incorporating more realistic dimensions and properties for the central protostar (placing them on the so-called "deuterium birthline"; cf. Stahler 1983; Shu & Terebey 1984; Palla & Stahler 1991), and, more important, by (2) adding an adjoining accretion disk. The disk plays two important roles: (1) it provides a rationale (rapid accretion) for understanding why a protostar might rotate near breakup in the first place, and (2) it gives an a priori reason for why the resulting magnetocentrifugally driven wind might have a preferred value (set by the disk accretion) for the mass-loss rate (see § 4.1). The latter constraint removes the uncertainty in the gas density at the sonic transition that occurs in HM's theory. When the base of the flow connects to a large reservoir of matter elsewhere, the sonic density adjusts itself to whatever value is required to keep the system in a quasi-stationary state. A formal derivation of the requirement of quasi-stationarity yields a wind mass-loss rate $\dot{M}_w$ directly proportional to the disk accretion rate $\dot{M}_D$ (see eq. [4.7a]):

$$\dot{M}_w = f\dot{M}_D \,. \tag{1.1}$$

SLRN estimated that $f \approx 0.3$ for a typical protostellar system. For definiteness, we suppose the central star to have properties (except possibly for rotation) similar to classical T Tauri stars (CTTSs). André et al. (1988, 1991) have detected and resolved by VLBI techniques circularly polarized radio emission from a young embedded star S1 of spectral type B3 in ρ Ophiuchus. They interpret their result in terms of nonthermal electrons radiating in an axisymmetric, possibly dipolar, magnetosphere extending over ~ 13 stellar radii and having a surface magnetic field of ~ 2 kG. Thus, our model may also apply to protostars and pre–main-sequence models of higher masses and luminosities (e.g., Herbig Ae and Be stars), but we consider it prudent to put off any discussion of these objects, whose magnetic properties are relatively unknown, until we have better understood the more intensively studied cases.

Figure 1 gives the basic physical picture of the modified SLRN model. We suppose that all rotating stars with extensive

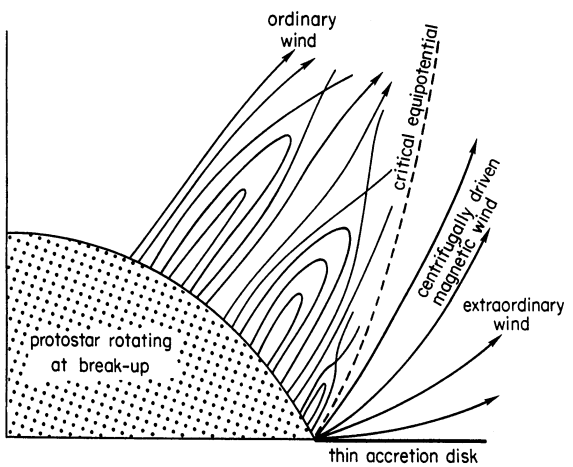

FIG. 1.—A complex geometry of open and closed field lines exists over most of the surface area of a protostar, with an ordinary wind (O-wind) blowing out along the open field lines. This wind intensifies into an extraordinary wind (X-wind) driven by magnetocentrifugal effects if open field lines protrude from the equatorial region of a star spun to breakup by heavy accretion from a thin accretion disk.

outer convection zones possess magnetically active surfaces having a complex network of open and closed field lines. An ordinary stellar wind (O-wind) blows along the open field lines. Over most of the stellar surface, the O-wind (perhaps Alfvén-wave driven) has to do work against almost the full gravitational field of a normal star. If open field lines emerge, however, from the equatorial regions of a star rotating nearly at breakup, then centrifugal effects may boost relatively cool gas even in the photosphere to launch speeds. The stellar wind may intensify in these regions to a much stronger outflow—an extraordinary wind (X-wind).

1.4. *T Tauri Stars as Slow Rotators*

Observations of optically revealed objects such as CTTSs show that they usually rotate at speeds an order of magnitude below breakup (Vogel & Kuhi 1981; Hartmann & Stauffer 1989; Bouvier 1990; Attridge & Herbst 1992, 1994; Bouvier et al. 1993). Yet CTTSs also possess reasonably strong winds. Edwards et al. (1993a) claim that CTTS winds empirically satisfy a relationship like equation (1.1), with $f \approx 0.1$, but this number contains considerable uncertainty (Edwards 1993, personal communication). They suggest that CTTS winds probably represent the lower end of the power spectrum of objects that include the drivers of bipolar molecular outflows. The observation that some T Tauri stars have well-collimated optical jets further strengthens this point of view. Taken together these observations motivate a unified approach for embedded sources and T Tauri stars that accomodates slow stellar rotation.

A naive modification of Figure 1, however, leads to its own difficulties. For example, suppose that the accretion disk does extend to the surface of a CTTS (as in the original models of "boundary layers" to explain ultraviolet excesses by Bertout 1987; Kenyon & Hartmann 1987; Bertout, Basri, & Bourier 1988), but that it manages to spin only a small equatorial band of the star to breakup. The open magnetic field lines in the equatorial band can then supply the X-celerator mechanism, while the rest of the slowly rotating star can produce the narrow photospheric lines. Unfortunately, Ekman pumping of stellar fluid to the boundary layer is an efficient mechanism when a disk abuts a fully convective star (Galli 1990), so the spinup of the entire stellar photosphere to angular velocities comparable to the equatorial value cannot be evaded for very long.

The search for a different unifying principle motivates us to reexamine the relationships among disk accretion, mass loss, and stellar rotation rate. The slow rotation of CTTSs, despite the accretion of matter of high specific angular momentum, appears to result from the interaction of a strongly magnetized star with a surrounding disk (Königl 1991; Edwards et al. 1993b). In §§ 2 and 3 we show that any spindown interaction involving accretion from a magnetically truncated disk has a natural consequence an X-celerator wind.

2. MAGNETIC INTERACTION OF A STAR AND A DISK

2.1. *Magnetic Spinup and Spindown*

Königl (1991) has invoked the theory of Ghosh & Lamb (1978, 1979a, b) to explain the slow rotation of T Tauri stars as the result of magnetic coupling to a truncated disk. Ghosh and Lamb suppose that the poloidal magnetic field of the star has a closed global structure, modeled approximately as an aligned dipole with magnetic moment μ_*. The magnetic field at the midplane therefore has a strength that decreases with increasing equatorial distance ϖ as

$$B = \frac{\mu_*}{\varpi^3} \equiv B_*\left(\frac{R_*}{\varpi}\right)^3 , \tag{2.1}$$

where B_* is the field strength at the star's equatorial radius R_*. Material at large disk radii ϖ which spirals slowly inward at an accretion rate $\dot{M}_D$ eventually climbs onto the closed field lines and is funneled at near free-fall speeds onto the star, truncating the disk at a distance $\varpi = R_t$ given by

$$R_t = \Gamma_t R_* , \tag{2.2a}$$

where Γ_t is the dimensionless parameter,

$$\Gamma_t \equiv \alpha_t\left(\frac{B_*^4 R_*^5}{GM_* \dot{M}_D^2}\right)^{1/7} , \tag{2.2b}$$

and α_t is a pure number of order unity introduced to allow the use of equal signs in the equations. Ghosh & Lamb (1979a) estimate $\alpha_t = 0.47$, whereas Arons (1986, 1993) in alternative calculations recommends $\alpha_t = 0.5$–1.

For parameters characteristic of CTTSs (see Bertout 1989 and § 2.7), equation (2.2b) yields Γ_t equal to 2–10. It may be no coincidence that the truncation radius R_t is only somewhat smaller than the transition radius for thermal ionization to provide good magnetic coupling calculated by Umebayashi & Nakano (1988). T Tauri stars with relatively low rates of mass accretion may naturally adopt quasi-stationary rotation rates Ω_* that correspond to corotation radii, $R_c \gtrsim R_t$ (see § 3.1), close to the maximum value where the disks still have appreciable electrical conductivity (see, however, § 3.2).

Ghosh & Lamb argue that the radius R_c where the Keplerian disk and the star corotate can substantially exceed R_t, although the excess can also be small in other circumstances. They claim that magnetic coupling to disk material interior to R_c tends to spin the star up, whereas coupling to disk material exterior to R_c tends to spin it down. Equilibrium arises when spin-up and spin-down tendencies are balanced.

There are two main difficulties with this picture. First, since stellar magnetic field lines thread parts of the disk that rotate at different angular speeds from the star (i.e., everywhere except at the single radius $\varpi = R_c$), the field configuration must constantly try to wrap up. To deal with this problem Ghosh & Lamb introduce diffusive instabilities to reconnect the field continually. While this may well happen, the uncertainty introduced in the theoretical calculations vitiates detailed predictions.

Second, unlike the material interior to R_c, which pours magnetically onto the star, the gas exterior to R_c cannot energetically climb the field lines to fill the space between the disk and the star. Coronal gas could conceivably act as a substitute for the current-carrying medium that mediates angular momentum transport between the disk and the star. However, interpretations of X-ray flare observations of T Tauri stars in terms of magnetic loop models (see the review of Montmerle et al. 1993) suggest plasma at temperatures of $\sim 10^7$ K and electron densities $n_e \sim 10^{10}$ cm^{-3} extending only over ~ 2 stellar radii, well within R_c. The spin-down torques associated with any closed field lines extending beyond R_c may therefore not be able to compete with the spin-up torques of those interior to R_c. Thus, it is an open question whether the Ghosh & Lamb mechanism can actually spin a CTTS down, rather than only spinning it up (the usual application in X-ray pulsars).

2.2. *Exclusion of Field from Disk Except for Corotating Parts*

To avoid the above problems, we assume that the magnetic field maintains a fixed pattern in a frame that rotates with the star. The stellar magnetic field will then try to exclude a conducting, differentially rotating, disk except for those parts that also corotate with the star. A real star will probably have both open and closed field lines (see Fig. 1), but while the former is associated with an O-wind, it is the interaction of the latter with the disk that most interests us here. We therefore focus on the case when the star left to itself has only a globally closed field. Arons (1986, 1987)—summarizing unpublished work by himself, McKee, & Pudritz—has provided the following thought experiment to help guide our ideas.

Imagine with Aly (1980) an infinitely conducting, nonaccreting, thin disk with an inner edge $R_t > R_*$ placed in the equatorial plane of a stellar magneton (a star with a pure dipole magnetic field if it existed in a vacuum). The magnetic field tries everywhere to thread vertically through the disk, but the diamagnetic properties of the disk plasma prevent such penetration. Shielding currents, in the form of circulating rings at each radius ϖ, automatically arise in the surface layers of the disk that generate a counter magnetic field canceling the normal component of the stellar contribution just above and below the disk. The total vector magnetic dipole moment of these induced disk currents must exactly equal but oppose the dipole distribution of the stellar currents, so that the net field vanishes as a quadrupole at large distances from the star or disk. However, in the space between the star and disk, the two contributions do not cancel exactly, and the total field assumes the configuration drawn in Figure 2*a*. The field attains the unperturbed stellar dipole value as we approach the star; but at a small distance s from the disk edge at R_t, it has a value that diverges as $s^{-1/2}$ when $s \to 0$.

In Aly's theory, the magnetic diffusivity η_D (due to resistivity and ambipolar diffusion), thickness H, and accretion rate $\dot{M}_D$ of the disk are all taken to be zero, and the magnetic field configuration is axisymmetric with respect to the disk (for his case $\chi = 0$). Under these conditions, no mechanical properties need be ascribed to the disk or star, and the disk's inner edge could have an arbitrary location R_t. However, if we imagine this situation to be the limiting case of less idealized conditions, we obtain additional considerations for the steady state problem. For example, we may regard the meridional plane of the star and inner edge of the disk to be threaded by one last (kinked) field line. For that field line not to be continuously wrapped up, the disk at R_t and the star must corotate with one another. To emphasize this constraint, we have marked the radius of the inner disk edge in Figure 2*a*, not by R_t, but by R_x.

We take R_x to be defined by where the natural Keplerian angular velocity of the disk,

$$\Omega_x = \left(\frac{GM_*}{R_x^3}\right)^{1/2}, \tag{2.3a}$$

equals the angular velocity of the star Ω_* (i.e., R_x is the radius previously denoted by R_c). The effective potential (centrifugal plus gravitational) associated with a frame of reference that rotates at $\Omega_x = \Omega_*$ is

$$V_{\rm eff} = -\frac{GM_*}{(\varpi^2 + z^2)^{1/2}} - \frac{1}{2}\Omega_x^2 \varpi^2 + \frac{3}{2}\Omega_x^2 R_x^2 . \tag{2.3b}$$

For convenience we have defined the arbitrary additive constant so that $V_{\rm eff} = 0$ at the X-point, $\varpi = R_x$ and $z = 0$, where the effective gravitational field vanishes, $-\nabla V_{\rm eff} = 0$. We easily verify that $\partial^2 V_{\rm eff}/\partial \varpi^2 < 0$, whereas $\partial^2 V_{\rm eff}/\partial z^2 > 0$ at the X-point; thus, $V_{\rm eff}$ plotted against (ϖ, z) has the shape of a saddle centered on the X-point.

When $\dot{M}_D \neq 0$ and $\eta_D \neq 0$ by finite amounts, the single radius $R_t = R_x$ broadens out to a whole region, with $R_t < R_x$

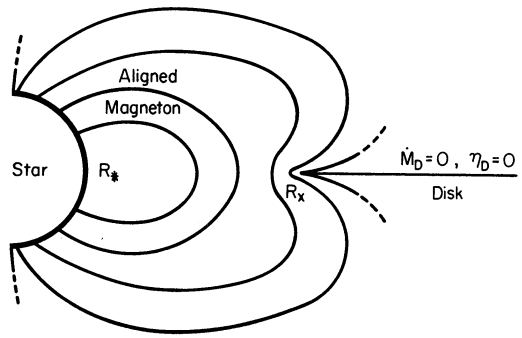

FIG. 2*a*

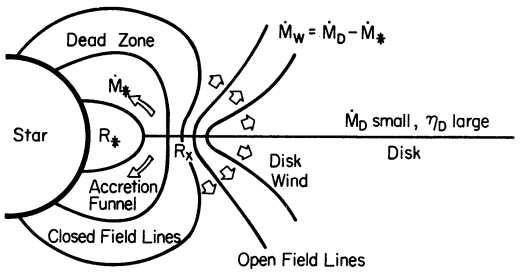

FIG. 2*b*

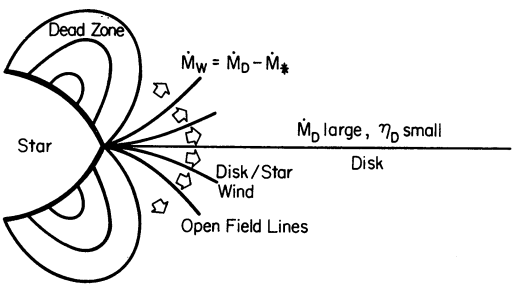

FIG. 2*c*

FIG. 2.—Schematic sequence in the interaction of an aligned stellar magneton and a surrounding disk. (*a*) The situation when a truncated disk has no inward motion due to accretion, $\dot{M}_D = 0$, and no magnetic diffusivity, $\eta_D = 0$. The field lines emerging from near the pole of the star connect at very large distances with field lines that skim radially above and below the disk, making a sharp turn (kink) to meet near a disk edge R_x assumed larger than the stellar radius R_*. (*b*) The situation with a small nonzero $\dot{M}_D$ and a finite (relatively large) η_D. Matter interior to the radius R_x diffuses onto field lines that bow inward and is funneled onto the star. Matter exterior to the radius R_x diffuses onto field lines that bow outward in an ideal configuration to launch a magnetocentrifugally driven wind. Since these field lines originally closed back to the star only by turning around at very large distances (where they are very weak), it is easy for the outflowing gas to make a transition to super-Alfvénic flow and to tear them open. The open field lines are then held in place in the equatorial plane by the inward press of the accretion flow and the outward press of the field lines still closed on the star and embedded in matter forced to rotate (slightly) faster than its natural Keplerian speed. (*c*) The situation with a large $\dot{M}_D$ and a finite (relatively small) η_D. The heavy inward flow of disk gas has pressed all the equatorial field lines onto the stellar surface, and the Keplerian motion of the adjoining disk forces the star to rotate at breakup. The magnetocentrifugally driven wind now becomes identical to the X-celerator model proposed by SLRN.

by a finite amount (see Fig. 2*b*). Since gravity and rotational inertia exactly balance at the X-point, we naturally expect matter in a thin disk (where the local isothermal sound speed $a_x \ll R_x\Omega_x$) to rotate at angular speed Ω_x at $\varpi = R_x$. In fact, the closed magnetic field lines, being dynamically strong (since by definition they truncate the disk at R_t), will enforce (near) corotation of the disk at the single angular velocity $\Omega_* = \Omega_x$ *throughout* the region between R_t and (slightly beyond) R_x where the disk is threaded by stellar or induced disk fields. On this essential point, we differ from Arons, McKee, & Pudritz, who considered—in the context of disks around X-ray sources—a boundary layer with much greater conductivity, shear, and turbulence than we ascribe to the threaded region.

2.3. *Funnel and Wind Flows*

Slightly exterior to R_t, in a zone that we call the T-region, the near-uniform rotation at sub-Keplerian speeds and the inward bowing of the closed field lines allow the gas energetically to climb onto the lines of $\boldsymbol{B}$ and fall onto the star. Under the assumption of field freezing, lines of $\boldsymbol{B}$ coincide with lines of $\boldsymbol{u}$ in a frame that rotates at Ω_*. The streamlines swirl inward as the accreting gas spins up. With respect to the direction of rotation, therefore, the field lines tug forward their footpoints in the disk and backward their footpoints in the star. This trailing-spiral configuration for the magnetic field leads to a consequent transfer of the excess angular momentum originally in the gas *from the star to the disk* (see § 2.6).

Slightly exterior to R_x, in a zone that we call the X-region, any closed field line rotating with the star would try to force the gas to super-Keplerian speeds. The outward bowing of these field lines naturally gives not inflow but outflow, i.e., a *disk wind* (Arons 1986, 1987; Camenzind 1990; Wardle & Königl 1993), if the field lines that would originally close by bending at very large distances back to the star can be opened by the ram pressure of the outflowing gas. The open field lines are pinned in place by a combination of the inward motion of the disk accretion (near the midplane) and the outward centrifugal fling associated with the super-Keplerian rotation (near the disk surface). Because the gas in the X-wind spins down as it moves outward, a field line projected into the equatorial plane again traces a trailing spiral (with respect to the sense of rotation in an inertial frame), but the footpoint of the field in the disk now lies at the *inner* terminus of the spiral so the magnetic torque of the X-wind acts to *remove* angular momentum from the X-region (see § 4.1 and Paper III).

Between the T-region (where angular momentum flows into the disk from the funnel flow) and the X-region (where angular momentum flows out of the disk into the X-wind) lies a dead zone (where the matter diffuses quasi-statically across field lines). In order for the diffusion of neutral gas to yield accretion, the specific angular momentum of the neutral gas either must be carried outward through the disk viscously (perhaps by the action of the Balbus-Hawley instability; see §§ 2.8 and 3.2), or must be imparted by neutral-ion collisions to the coronal plasma tied to the closed field lines. As in the Ghosh & Lamb picture (except that the pattern of field lines rotate uniformly and do not wrap up), the latter possibility would torque up the star since the neutrals in the disk for $R_t < \varpi < R_x$ have a natural tendency to rotate faster than the stellar field lines and the ions that are attached to them. In what follows, we assume that the former possibility dominates—i.e., that there exists an internal mechanism in the disk that takes the excess angular momentum deposited to the disk at R_t and transports it through the dead zone of the disk to R_x, where it can be carried away (mostly) by the induced X-wind (see § 4.1).

Figure 3 depicts schematically what happens around and between the X- and T-regions. The gas enters the region from the right as a slow viscous accretion flow. The relatively high magnetic diffusivity near the midplane allows the gas to drift across field lines. The outward bowing of the field lines to the right of the X-point cause streamlines at high disk latitudes to deflect away from the midplane (see Wardle & Königl 1993 for a calculation of the effect), eventually making a transition from subsonic to supersonic flow (in the corotating frame of reference) at the sonic surface (dotted curves that asymptote to the outer [right] branch of the critical equipotential). The relatively large ionization fractions at low densities allow good magnetic coupling, and the streamlines turn parallel to the field lines, launching the now outwardly moving gas into a magnetocentrifugally driven wind.

As the streamlines are peeled off one by one heading from R_x to R_t, the surface density drops relative to its inlet value. This reduces the amount of accretion curvature that the midplane fields will acquire, i.e., the field lines make a natural transition to the opposite kind of curvature (bowing in toward the star). As the gas closer to the midplane climb onto these field lines, it also makes a sonic transition (at the dotted curve that asymptote to the inner [left] branch of the critical equipotential) and is funneled as supersonic (but sub-Alfvénic) flow onto the star (well to the left off the page of the diagram). This happens when the field lines bow inward marginally more quickly than does the corresponding effective equipotential, a configuration that Scharleman (1978) and Aly (1980) refer to as a "lip." For the rotating analogue of the aligned magnetosphere in Aly's solution, the lip of the funnel in the midplane occurs at $\varpi = 0.72R_x$, where the distorted field has a strength only 50% larger than

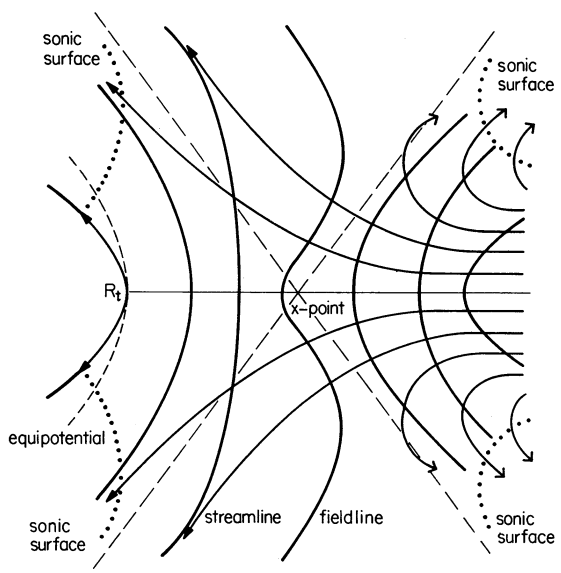

FIG. 3.—Schematic depiction of the meridional flow of imperfectly conducting gas from the X-region to the *T*-region (not to scale). *Dashed curves* give contours of constant effective potential (gravitational plus centrifugal), with the dashed "X" marking the critical equipotential; *heavy solid curves with arrows* depict streamlines; *light solid lines* show magnetic field lines; and *dotted curves* correspond to loci where the gas makes a transition from subsonic to supersonic flow. Beyond the sonic surfaces, centrifugal excesses and deficits (when the angular speed of rotation is kept by magnetic stresses equal to Ω_x within order ϵ^2) accelerate the gas in the sectors to the right and left of the dashed "X" to fast wind and funnel flows.

the unperturbed stellar dipole. The wind and funnel flow will modify the magnetic field solution appropriate for the vacuum case. When a wind exists, the outermost *closed* field lines do not completely wrap around a thin disk, so less "unbending" is required at small radii to permit a funnel flow. Thus, we anticipate that the funnel flow will become fully dynamical at a closer distance to R_x than the nominal 28% figure given by Aly's solution.

In particular, if transport through the dead zone proves to be inefficient, then the angular momentum deposited into the disk by the funnel flow would cause the material in the T-region, *and the field lines to which it is attached*, to move outward toward the X-point. Conversely, the material at the footpoint of the open fields in the wind region would be torqued *down* by the wind flow, and it would move inward also toward the X-point. Thus, in the absence of efficient dead-zone torques, there may exist a tendency of field lines throughout the dead zone on both sides of the natural corotation radius to pinch toward the X-point. In this case, R_t and R_x would be separated only by a small distance, and the angular momentum transport radially through the dead zone may then all occur in an ϵ-neighborhood of the X-point (see eq. [2.4b] below).

Eventually, when the gas nears R_t, almost all of the streamlines traveling in the disk plane will have been off-loaded (either to the wind or to the funnel flow), and the field goes to an essentially force-free configuration. For an idealized calculation of the aligned dipole configuration, the streamline exactly on the midplane comes to a stagnation point at $\varpi = R_t$, where the field line has a "lip" with respect to the effective equipotential. At R_t, the streamline bifurcates (taking the form of a sideways "T"), with the gas accelerating from rest at the stagnation point and contributing to two funnel flows that eventually impact the star on its two opposite hemispheres. Some low-density gas may exist in the stellar magnetosphere even to the left of the fiducial "stagnation" streamline, but the amount cannot be large if the diffusive timescale for the disk to supply this gas is long compared to the dynamical timescale for the funnel flow to empty the region.

The inward and outward bifurcation of streamlines at high latitudes in the upper and lower sectors of the X-geometry of the effective potential leaves only rarefied subsonically moving gas that connects to a (quasi-static) dead zone threaded by closed magnetic fields in pressure equilibrium with the funnel and wind flows (see Fig. 4). Although these lightly loaded field lines are essentially force-free well above and below the disk, they are probably not force-free within the disk. Indeed, the inward (near the midplane) and outward (above and below the midplane) excursions of the gas may introduce sideways-W–shaped field lines that bend much more severely than indicated by the one such shaped field line near the X-potential in Figure 3. Such W-shaped field lines would tend to enforce near-rigid rotation of the gas in the disk portion of the dead zone. If the radial excursion of the connected field lines becomes comparable to the separation between R_t and R_x, then the Balbus-Hawley-Wardle-Königl mechanism (see § 2.8) may effect a direct transfer of angular momentum from the T-region to the X-region across the nominal dead zone. We speculate that the relatively large amounts of magnetic diffusivity and small amounts of shear of the present problem prevent reconnection from chopping the radially stretched field lines into many small magnetic loops (see Hawley & Balbus 1991, 1992) that would drastically decrease the efficiency of this angular momentum transport mechanism in the disk.

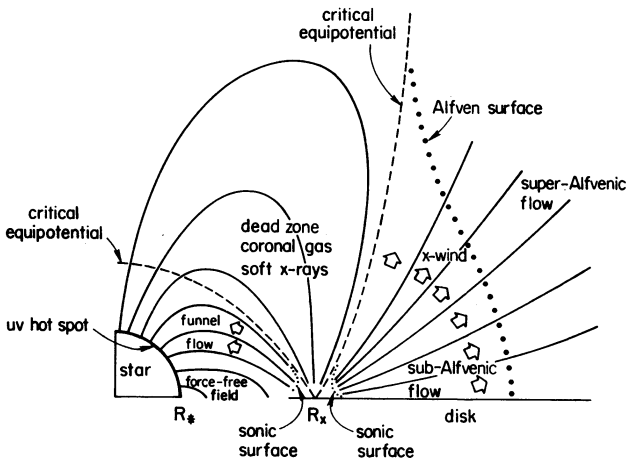

FIG. 4.—Schematic diagram of principal components in a typical CTTS system.

If the true situation corresponds to a sufficiently *tilted dipole* rather than a completely aligned one, the truncation radius R_t may become virtually indistinguishable from the nominal corotation radius R_x. In this case, except for some pinching, a dipole field line tilted radially *outward* by more than 30° from the vertical above the midplane, which is good for launching a wind flow, on passing through the midplane becomes tilted radially *inward* by more than 30° from the vertical below the midplane, which is good for launching a funnel flow. In this situation, the dead zone may be small or nonexistent, and excess angular momentum transported magnetically from the star to the disk by the funnel flow can be directly carried away by the wind. At 180° difference in longitude on the other side of the disk, the sense of outflow (below the midplane) and inflow (above the midplane) reverses, so we anticipate that such a configuration would exhibit a periodicity in outflow and inflow properties that would (1) equal the spin period of the star, and (2) have a definite phase difference with respect to each other. (See the discussion in § 5.2 on SU Aur.)

The outer branch of the critical equipotential turns asymptotically parallel to z at a cylindrical distance $\varpi = 3^{1/2}R_x$ from the rotation axis. A current sheet on the locus of the outer branch of the critical equipotential, defined by $V_{\rm eff}(\varpi, z) = 0$, therefore offers an attractive separatrix between open field lines and closed ones, i.e., a distinction between gas energetically capable of outward magnetocentrifugal flinging and gas incapable of such motion. Shielding currents must also lie at the interface between the disk surface and the wind streamlines that skim just above and below the disk, with the magnetic pressure in the wind compressing the disk in the vertical direction to a level that can be resisted by the internal gas pressure (cf. Wardle & Königl's 1993 analogous description of the "pinch effect" of oppositely bent field lines on either side of the midplane).

2.4. *Estimate of the Size and Field of the X-Region*

With the above mental picture, we now demonstrate that the X-region, where the induced disk-wind originates, has a fractional size $\Delta\varpi/R_x$ of order $\epsilon \equiv a_x/R_x\Omega_x$, where a_x is the (isothermal) speed of sound. (For the observed parameters of T Tauri stars, $\epsilon \lesssim 0.05$.) In the X-region, the net centrifugal accelerations, above those needed for balance against gravity, have excesses of order $\Omega_x^2\Delta\varpi$. For these accelerations to yield differential fluid speeds of order a_x in a crossing time of order $\Delta\varpi/a_x$

requires

$$(\Omega_x^2 \Delta\varpi)(\Delta\varpi/a_x) \sim a_x ; \tag{2.4a}$$

i.e.,

$$\frac{\Delta\varpi}{R_x} \sim \frac{a_x}{R_x \Omega_x} \equiv \epsilon , \tag{2.4b}$$

which is the desired result. Equation (2.4b) states that the X-region has a width $\Delta\varpi$ comparable to the vertical scale height of the local disk gas, $H_x = a_x/\Omega_x$.

The crossing time $\Delta\varpi/a_x \sim \Omega_x^{-1}$ is even shorter in our problem than that of Wardle & Königl (1993). The short timescale presents no difficulties in the present context because (*a*) we envisage a large accreting reservoir of matter beyond R_x that can maintain a nonzero surface density at the X-region despite the rapid wind (and transition to funnel) flow out of it, (*b*) the large curls of the magnetic field that drive the wind flow do not arise from any intrinsic properties of magnetism in the disk, but rather from the presence of the stellar field and the innate tendency of the disk to develop shielding currents that try (imperfectly) to prevent the field's penetration.

The strength of the magnetic field makes no appearance in the formula (2.4b) once we have taken into account its tendency to enforce nearly uniform rotation in the X-region. We may use conventional MHD (where we need not think about currents at all) to derive an estimate of this strength by approaching the problem with finite conductivity from the limit of zero ionization. For a completely neutral disk, the unperturbed dipole field of the star may thread the disk with impunity. As we turn up the ionization in the surface layers (and the midplane for small ϖ), the disk accretion sweeps inward the outer field lines. In order of magnitude, the net effect in steady state is as if we bunched all the original field lines from $2R_x$ to R_x (where we think of the field as pinned) into a thin annulus of width ϵR_x. Clearly, the field strength B_x in the general X-region would then increase above the vacuum dipole value $B_*(R_*/R_x)^3$ by roughly a factor $1/\epsilon$.

Thus, the magnetic field in the X-region is actually much larger (by the factor ϵ^{-1}) than needed to modify the Keplerian kinematics of the local gas by a slight amount. In fact, the field is strong enough to keep the gas in the entire region *nearly* uniformly rotating in the following mathematical sense: referred to the corotating frame, the nondimensional fluid velocity in the azimuthal direction, $u_\varphi/R_x\Omega_x$, is of order ϵ^2 in the X-region (see § 2.6), when Keplerian shear across a region of fractional size ϵ would have led us to expect it to be of order ϵ (see also Paper II). The field in the X-region exceeds Aly's value at R_x by a factor of $\epsilon^{-1/2}$ because the accretion flow from the outer disk pushes up against field embedded in reasonably dense gas just outside R_x that has been forced to rotate faster than required for balance against gravity, whereas in Aly's solution the insertion of the disk has only to push against vacuum fields that distribute the load (in the absence of a pinch) more continuously to the interior.

2.5. *Location of the X- and T-Points*

Consider now the dynamics of the wind flow. At the top and bottom sonic surfaces, each of which has an area $2\pi\varpi\Delta\varpi$, gas of density ρ_{sx}, moving at the isothermal sound speed $a \sim \epsilon\varpi\Omega_*$, carries a wind-loss rate $\dot{M}_w$ comparable in order of magnitude to the disk accretion rate $\dot{M}_D$. Thus, we require

$$4\pi\epsilon\rho_{sx}\varpi^2\Omega_*\Delta\varpi \sim \dot{M}_w . \tag{2.5a}$$

With $\varpi = R_x$ and $\Delta\varpi \sim \epsilon R_x$, the sonic density in the X-region then reads

$$\rho_{sx} \sim \frac{\epsilon^{-2}\dot{M}_w}{4\pi\Omega_x R_x^3} . \tag{2.5b}$$

After the sonic transition, the gas accelerates to speeds of order $\varpi\Omega_*$, with the flux tubes and stream tubes in the X-wind spreading out by a factor $\varpi/\Delta\varpi$. Thus, to satisfy mass continuity, the density ρ in the wind must decrease in comparison with ρ_{sx} by a factor of order $(a/\varpi\Omega_*)(\Delta\varpi/\varpi) \sim \epsilon^2$. At the reduced density $\rho \sim \epsilon^2\rho_{sx}$, the Alfvén speed $B/(4\pi\rho)^{1/2}$ associated with the unpinched stellar magnetic field $B \sim \epsilon B_x$ must remain at least comparable to $\varpi\Omega_x$ if the X-region field is to fling the gas into an escaping wind. This constraint implies

$$B_x \sim \epsilon^{-1}\left(\frac{\dot{M}_w\Omega_x}{R_x}\right)^{1/2} . \tag{2.5c}$$

The uncompressed field ϵB_x must have strength comparable to the unperturbed stellar dipole, $B_*(R_*/R_x)^3$. The substitution of equation (2.5c) now yields the identification,

$$R_x = \Gamma_x R_* , \tag{2.6a}$$

$$\Gamma_x = \alpha_x(B_*^4 R_*^5/GM_*\dot{M}_D^2)^{1/7} , \tag{2.6b}$$

where α_x is a pure number of order unity that absorbs the uncertainties of the detailed disk-magnetospheric interactions as well as the substitution of $\dot{M}_D$ for $\dot{M}_w$.

Except for the replacement of the subscript x for the subscript t, equations (2.6a)–(2.6b) recover the Ghosh & Lamb type of formulae (cf. eqs. [2.2a]–[2.2b]). We therefore have the following important conclusion: any stellar field strong enough to truncate the disk at R_t and to convert the disk-accretion flow at a rate $\dot{M}_D$ to a funnel flow at a rate $\dot{M}_*$ *automatically has sufficient strength* to drive an X-wind from R_x somewhat beyond R_t, at a rate $\dot{M}_w = \dot{M}_D - \dot{M}_*$ comparable to both $\dot{M}_*$ and $\dot{M}_D$. In a future communication we will address the question of the distance between R_t and R_x.

2.6. *Role of Nearly Uniform Rotation in Angular Momentum Transport*

The T-region being in nearly uniform rotation has an important consequence for the sense of magnetic torques associated with the funnel flow. If we adopt the assumption of field freezing for the dynamically moving gas (see § 3.1), we can show that $\boldsymbol{B} = \beta\rho\boldsymbol{u}$ in a frame that rotates with angular velocity $\Omega_* = \Omega_x$, where β (with opposite signs for the outflows above and below the disk) is a constant on a streamline; i.e., $\beta = \beta(\psi)$, where ψ is the streamfunction for steady, axisymmetric, compressible flow (see Paper II). Consider the flow of gas in the direction $\hat{\boldsymbol{n}}$. The sum of the z-component of the specific angular momentum (in an inertial frame) carried in the gas $\varpi(\varpi\Omega_* + u_\varphi) \equiv j_g$ and in the field (Maxwell torque divided by mass flux) $-\varpi B_\varphi \boldsymbol{B}\cdot\hat{\boldsymbol{n}}/4\pi\rho\boldsymbol{u}\cdot\hat{\boldsymbol{n}} = -\varpi\beta^2\rho u_\varphi/4\pi \equiv j_B$ is also conserved on a streamline: $j_g + j_B = j(\psi)$, where $j(\psi)$ is some fixed function. Thus, we have

$$\varpi^2\Omega_* + \varpi\left(1 - \frac{\beta^2\rho}{4\pi}\right)u_\varphi = j(\psi) , \tag{2.7a}$$

which is the dimensional form of equation (2.13a) of Paper II, but now applied to the T-region instead of the X-region.

The quantity $\beta^2\rho/4\pi = |\boldsymbol{B}|^2/4\pi\rho|\boldsymbol{u}|^2$ represents the inverse square of the Alfvén Mach number in the corotating frame and

is greater than unity for sub-Alfvénic flow. Thus the term $(1 - \beta^2\rho/4\pi)u_\varphi$ is negative throughout the entire funnel flow, if the flow remains sub-Alfvénic and the inward heading gas spins up in the sense of rotation (i.e., if $u_\varphi \geq 0$). Field lines are then trailing spirals. On the other hand, the magnetic field becomes very strong near the surface of the star. If it dominates the motion of the gas, the field lines at the surface of the star will have little azimuthal component B_φ (because a pure dipole has none), and we expect $u_\varphi \propto B_\varphi$ also to be small on impact with the star. Then the second term in equation (2.7a) is not much larger than the first, unless the inflow is extremely sub-Alfvénic. In any case, the sign of the second term opposes the first, so a conservative approach approximates $u_\varphi = 0$ on the star to obtain an evaluation of $j(\psi)$:

$$j(\psi) \approx \varpi_*^2 \Omega_* , \tag{2.7b}$$

where $\varpi_*(\psi)$ is the axial distance of the streamline labeled by ψ when it strikes the star. The square of the radius where the same streamline originates in the disk, $\varpi_D^2(\psi) \approx R_t^2$, is typically larger than $\varpi_*^2(\psi)$ by one or more orders of magnitude; hence $j(\psi) \ll R_t^2\Omega_*$ for each streamline in the funnel flow. Since the net flux of angular momentum into the star is given by $j\rho\boldsymbol{u} \cdot \hat{\boldsymbol{n}}$, we see that this flux is much less than the mass flux times the specific angular momentum at the launch point in the disk (the usual assumption in spin-up arguments for X-ray pulsars).

The difference with the standard assumption arises because the back torque exerted on the disk by the field $\propto -j_B = \varpi\beta^2\rho u_\varphi/4\pi \approx (\varpi_D^2 - \varpi_*^2)\Omega_x$ is *positive* and transfers angular momentum from the star to the X-region of the disk by roughly the amount required to account for the difference in their specific moments of inertia, i.e., as to leave them corotating with each other if we've set up the steady state problem correctly. We cannot overemphasize the importance of the last conclusion, which differs in *sign* from the conventional belief on the basis of the theory of Ghosh & Lamb.

2.7. *Some Numerical Estimates*

In a full calculation, the demand of quasi-stationarity of the global problem presumably determines the precise value of α_x. In other words, the stellar rotation rate $\Omega_* = \Omega_x$ is an eigenvalue of a steady state calculation that examines the details of the flow of mass and angular momentum onto the star. In the absence of such a complete theory, we adopt the value $\alpha_x = 1$. For $M_* = 0.5\ M_\odot$, $R_* = 2.3\ R_\odot$, $B_* = 1500$ G, and $\dot{M}_D = 1 \times 10^{-7}\ M_\odot\ \mathrm{yr}^{-1}$ (see Bertout 1989), equation (2.6b) yields $\Gamma_x = 5.7$. The corresponding rotation speed and period are $R_x\Omega_x = 85\ \mathrm{km\ s^{-1}}$ and $2\pi/\Omega_* = 2\pi/\Omega_x = 8$d. A period of 8d is indeed typical of T Tauri stars with stellar effective temperatures $T_* < 4500$ K (see Edwards et al. 1993b; Bouvier et al. 1993).

At a distance $R_x = \Gamma_x R_*$, we estimate the disk temperature T_x as (cf. eq. [A22] of Adams et al. 1988 and eq. [7.24] of Shu 1992; see Calvet et al. 1991 for a more sophisticated treatment):

$$T_x = \left\{ \frac{T_*^4}{\pi} \left[\arcsin\left(\Gamma_x^{-1}\right) - \Gamma_x^{-1}\left(1 - \Gamma_x^{-1}\right)^{1/2} \right] + A\,\frac{GM_*\dot{M}_D}{4\pi\sigma_{SB}R_x^3} \right\}^{1/4} , \tag{2.8}$$

where σ_{SB} is the Stefan-Boltzmann constant. The first and second terms inside the braces represent, respectively, the contributions from reprocessing and accretional heating. In a standard viscous accretion disk, $A = 3/2$; however, the shear rate in the X-region is a factor ϵ smaller than the Keplerian value in our theory, and ambipolar diffusion and ohmic dissipation may dominate the actual accretion heating, in which case § 3.1 also estimates $A \sim \epsilon$. With $T_* = 4500$ K and the other parameters given as before, equation (2.8) yields $T_x = 1100$ K for $A = 3/2$ (with most of the contribution coming from the accretional heating term), while $T_x \sim 850$ K for $A = \epsilon \sim 0.02$ (with most of the contribution coming from the reprocessing term).

Equation (2.8) gives the temperature of the surface of the disk at R_x. If the disk is optically thick to its own thermal radiation, the midplane temperature is given by a similar formula except the term proportional to A is multiplied by τ_0, the Rosseland-mean optical depth from the surface to the midplane. Even when we know the surface density of the disk σ_x (see eq. [2.11] below), however, uncertainties in the correct nebular dust opacities make estimates for τ_0 highly speculative. Theory assuming perfect sticking of particles (see, e.g., Fig. 10 of Weidenschilling & Cuzzi 1993) suggests that dust settling and agglomeration should occur very quickly even in a turbulent nebular disk, reducing τ_0 from initial values $\gtrsim 10^3$ to values $\lesssim 1$ in only thousands of orbital periods ($\lesssim 10^4$ yr). On the other hand, observation of the infrared spectral energy distributions of T Tauri disks suggests that their inner parts must remain optically thick for 10^6–10^7 yr (see, e.g., Strom et al. 1989). Evidently, processes such as collisional fragmentation or continued infall and radial drift must resupply a population of small grains that maintain $\tau_0 > 1$. In what follows, we suppose that moderate variations 1100 K yield reasonable values for T_x at the surface and midplane of the X-region of the disk. The corresponding sound speed $a_x = 2\ \mathrm{km\ s^{-1}}$ for cosmic gas of a molecular composition yields $\epsilon_x = 0.024$.

With the same choice of other parameters, disk accretion rates higher than $4 \times 10^{-5}\ M_\odot\ \mathrm{yr}^{-1}$ (e.g., during a FU Orionis outburst; see Hartmann et al. 1993) would formally push R_x inside the surface of the star. The Keplerian part of the disk would then abut the stellar surface. After the passage of some transients, Ekman pumping would cause the photospheric and subphotospheric layers of the star to rotate at breakup with $R_x = R_*$.[1] The large stellar pressures would make the inner sonic surface (and the associated accretion funnel) disappear. There would then be no hot "boundary layer" and ultraviolet excesses associated with an accretion shock as it encounters the stellar surface. Thus, the high disk accretion limit of Figure 2*b* leads to Figure 2*c*, which is the original X-celerator model of SLRN. Figure 1 of SLRN therefore differs from Figure 1 of the present paper, mainly in that the latter allows the possibility of the a priori existence of open stellar field lines and ordinary stellar winds. As we shall see in Papers II and III, however, the properties of the X-wind do not depend on this distinction as long as we are free to specify the initial loading of mass on open field lines rooted in the X-region.

[1] Lee Hartmann (1993, personal communication) points out to us, however, that insufficient mass may be dumped onto the star per event to cause the entire star to spin at the break-up rate. In this situation, the frictional rubbing of the slower-spinning lower layers with the faster-spinning upper layers may result in as much as half of the accretional energy being dumped deep inside the star, where it ultimately emerges spread out over the entire stellar surface, rather than in a narrow boundary layer. Such a picture would represent a compromise between the view of Herbig (1977), according to whom an FU Orions outburst occurs in a star, and that of Hartmann et al. (1993), according to whom it occurs in a disk.

2.8. *Midplane versus Sonic Transition Densities in the X-Region*

The equation of motion implies that the Lorentz force per unit mass $(4\pi\rho)^{-1}(\nabla \times \boldsymbol{B}) \times \boldsymbol{B}$ equals the difference in acceleration produced by inertial, gravitational, and gas pressure effects. In order of magnitude, this acceleration yields at every vertical level the centrifugal excess that we associate with the X-region:

$$\left|\frac{1}{4\pi\rho}(\nabla \times \boldsymbol{B}) \times \boldsymbol{B}\right| \sim \Omega_x^2 \Delta\varpi \sim \Omega_x a_x \,. \tag{2.9a}$$

The nature of the approximate force balance, equation (2.9a), is very different for the matter at the sonic transition of the X-wind and for the deeper layers near the midplane. At the sonic transition the gas kinetic and ram pressures are low (order unity) compared to the magnetic stresses (order ϵ^{-2}), so that the fields must assume a nearly force-free configuration (see Paper II and III). At the midplane, the fields have unavoidable curvature and cannot be force-free (see Fig. 3). The Lorentz acceleration there has its natural scale:

$$\left|\frac{1}{4\pi\rho}(\nabla \times \boldsymbol{B}) \times \boldsymbol{B}\right|_0 \sim \frac{B_x^2}{4\pi\rho_0 H_B} \,, \tag{2.9b}$$

where H_B and ρ_0 represent the radius of curvature of the field and the density at the midplane. On the other hand, equations (2.5b) and (2.5c) imply that the magnetic stress (but not its divergence) has the same approximate strength at the midplane as it does at the sonic surface:

$$B_x^2/4\pi \sim \epsilon^{-2}\rho_{sx} a_x^2 \,; \tag{2.10a}$$

thus, equating equations (2.9a) and (2.9b) yields the density ratio:

$$\frac{\rho_0}{\rho_{sx}} \sim \epsilon^{-2}\left(\frac{H_x}{H_B}\right) , \tag{2.10b}$$

where we have written a_x/Ω_x as the usual isothermal scale height H_x. Since equations (2.10a)–(2.10b) imply that $\rho_0 a_x^2$ is greater than $B_x^2/4\pi$ by a factor $\sim H_x/H_B$, magnetic "pinch" forces associated with the reversal of strong fields across the midplane play less of a role for us than for Wardle & Königl (1993) in reducing H_B relative to H_x. To emphasize that the flow does have the freedom to adjust the field structure, however, we continue to retain the dependence on H_B, although we expect numerically that $H_B \sim H_x$.

Disks with central gas pressure $\rho_0 a_x^2 \gtrsim$ the magnetic pressure $B_x^2/8\pi$ of field lines threading vertically through the midplane are prone to the magnetocentrifugal instability discussed by Balbus & Hawley (1991, 1992) and Hawley & Balbus (1991, 1992) if $d\Omega/d\varpi < 0$. Because the shear rate is small and because we have a lightly ionized medium, however, we speculate (see the discussion of § 2.3) that the manifestation of the instability in the present circumstances produces steady counterstreams of neutral gas (as in Wardle & Königl's [1993] calculations), which gain or lose angular momenta with ions through collisions without tangling the vertical fields so badly as to cause them to disconnect from the star. Material with a deficit of angular momentum then moves toward the T-region where it can be dynamically funneled onto the star, and matter with an excess moves toward the X-region where it can be dynamically flung into a wind.

From equations (2.5b) and (2.10b), we get the surface density $\sigma_x \sim 2H_B\rho_0$ in the X-region:

$$\sigma_x \sim \frac{\epsilon^{-3}\dot{M}_w}{2\pi\Omega_x R_x^2} \,. \tag{2.11}$$

For $\dot{M}_w = 3 \times 10^{-8}\ M_\odot\ \mathrm{yr}^{-1}$, $R_x = 13\ R_\odot$, $2\pi/\Omega_x = 8$d, and $\epsilon = 0.024$, equations (2.5b), (2.5c), and (2.11) yield $\rho_{sx} \sim 4 \times 10^{-11}\ \mathrm{g\ cm^{-3}}$, $B_x \sim 180$ G, and $\sigma_x \sim 3 \times 10^3\ \mathrm{g\ cm^{-2}}$. This value of σ_x is one and a half orders of magnitude lower than the surface density, $\sim 1 \times 10^5\ \mathrm{g\ cm^{-2}}$, of a minimum solar nebula, extrapolated on a $\varpi^{-3/2}$ power law (Hayashi et al. 1985) from the region of planet formation to $13\ R_\odot$.

3. THE ROLE OF FINITE MAGNETIC DIFFUSIVITIES

Although finite diffusivities—viscous (ν_D) and magnetic (η_D)—play important roles in our conceptual thinking, they do not enter explicitly in any of the formulae derived in § 2. They affect primarily the determination of the viscous torque (see § 4.1), the degree to which streamlines coincide with field lines, the midplane radius of curvature H_B of the magnetic field, and the detailed physical properties of the dead zone and T-region. In particular, the part of our theory dealing with the magnetohydrodynamics of X-winds is sensitive only to certain very general assumptions about the effective magnitudes of ν_D and η_D.

3.1. *Microscopic Mechanisms*

For temperatures above 600 K, coupling to magnetic fields occurs through ions and electrons rather than charged grains (Umebayashi & Nakano 1988). The main mechanisms for producing charged particles in the surface layers of the X-region are thermal ionization of metal atoms and photoionization of hydrogen and carbon. To begin, we assume that ambipolar diffusion (rather than, say, turbulent viscosity or ohmic dissipation) sets the drift speed v_d of gas across field lines that remain spatially fixed in a corotating frame of reference. From equation (27.8) of Shu (1992),

$$v_d = \frac{1}{4\pi\gamma_{in}\rho_i\rho}\,|(\nabla \times \boldsymbol{B}) \times \boldsymbol{B}| \,, \tag{3.1}$$

where γ_{in}, the drag coefficient between ions and neutrals of mass densities ρ_i and ρ, has a value $\sim 3 \times 10^{13}\ \mathrm{cm^3\ g^{-1}\ s^{-1}}$ if the typical neutral species is H or H_2 and the typical ion is Na^+ or K^+. Substitution of the formula (2.9a) into equation (3.1) now yields for the drift speed at every vertical level in the X-region,

$$v_d \sim (\Omega_x t_{ni}) a_x \,, \tag{3.2a}$$

where we have defined

$$t_{ni} \equiv \frac{1}{\gamma_{in}\rho_i} \tag{3.2b}$$

as the mean collision time of a neutral atom in a dilute sea of ions. The latter is much larger in a lightly ionized medium than $t_{in} \equiv (\gamma_{in}\rho)^{-1}$, the mean collisional time of an ion in a dense sea of neutrals.

Equation (3.2a) has the following microscopic interpretation. Since ions are frozen by assumption to field lines that corotate with the star, they cannot move perpendicular to $\boldsymbol{B}$ (but see below for the situation near the midplane). At radii $\varpi > R_x$ by an amount $\Delta\varpi \sim \epsilon R_x$, the Keplerian speed differs

from the corotation rate $\varpi\Omega_x$ by an amount $\sim a_x$. Collisions with ions prevent neutrals from having this full velocity difference to the extent that the collision time t_{ni}, is shorter than the inverse Ω_x^{-1} of the orbital frequency (i.e., $v_d \ll a_x$ if $\Omega_x t_{ni} \ll 1$ in eq. [3.2a]). Away from the midplane, the collisions between the ions and neutrals tend to transfer angular momentum to neutrals from the more rapidly rotating ions (for $\varpi > R_x$) and therefore to help launch the neutral gas magnetocentrifugally into an outflowing wind. The opposite transfer of angular momentum occurs *on average* for $\varpi < R_x$; in this case the neutral gas is magnetocentrifugally torqued down (both in the dead zone and in the T-region). Near the midplane, the removal of gas in the T-region leads to negative gradients of magnetic and gas pressures that point inward, i.e., in a direction that helps to boost the gas into funnel flow. The steep *horizontal* structure and the near uniform rotation of the X- and T-regions (especially if they are pinched together) distinguish our problem from the one considered by Wardle & Königl (1993).

The volumetric contribution of ambipolar diffusion to the local heating equals $\gamma_{in}\rho\rho_i v_d^2$ (see eq. [27.18] of Shu 1992). If we use equations (3.2a)–(3.2b) to write $\gamma_{in}\rho_i v_d \sim \Omega_x a_x$, we get upon integrating over the vertical thickness of the disk,

$$\int_{-\infty}^{+\infty} \gamma_{in}\rho\rho_i v_d^2\, dz \sim \Omega_x a_x \frac{\dot{M}_D}{2\pi R_x}, \tag{3.3a}$$

where we have identified

$$\int_{-\infty}^{+\infty} \rho v_d\, dz \sim \frac{\dot{M}_D}{2\pi R_x}. \tag{3.3b}$$

Substituting $a_x = \epsilon R_x \Omega_x$ and $\Omega_x^2 = GM_*/R_x^3$, we find that the ambipolar-diffusion heating rate per unit area in the X-region is

$$\int_{-\infty}^{+\infty} \gamma_{in}\rho\rho_i v_d^2\, dz \sim \epsilon \frac{GM_*\dot{M}_D}{2\pi R_x^3}, \tag{3.4}$$

which leads to the identification $A \sim \epsilon$ in equation (2.8). With $A \ll \frac{1}{2}$, unlike the viscous case, most of the gravitational energy released by diffusive accretion goes into the driving of an X-wind, rather than into a heating of the local disk (see § 4.3).[2]

If only sodium and potassium are ionized (and completely so), then $\rho_i \sim 3 \times 10^{-5}\rho$. With $\rho = \rho_{sx} \sim 4 \times 10^{-11}$ g cm^{-3} and $2\pi/\Omega_x \sim 8$d, we obtain $v_d^{(s)}/a_x \sim 3 \times 10^{-4}$, making field freezing indeed a very good approximation for the dynamical part of the problem. Nevertheless, once wind speeds approach $R_x\Omega_x$ and the magnetic fields are no longer approximately force-free, frictional drag associated with ambipolar diffusion in an optically thin medium will raise the temperature above the value T_x estimated from equation (2.8) with $A \sim \epsilon$. This heating will be especially important at the relatively low densities associated with the outer parts of T Tauri winds (Natta, Giovanardi, & Palla 1988; Natta & Giovanardi 1990; Safier 1993) and may produce additional ionization. The gas in the funnel and wind flows will also be subject to the ultraviolet radiation from the magnetic "hot spots" on the star as well as the soft X-rays known empirically to exist for both classical and weak-lined T Tauri stars (Montmerle et al. 1993; Feigelson et al. 1993; see also Fig. 4).

The characteristic surface density, 3×10^3 g cm^{-2}, that we obtained in § 2.7 for the X-region suffices to shield the midplane against most forms of external ionizing radiation. The midplane gas should then be exceedingly neutral for midplane temperatures T_x between 1000 and 1500 K (cf. § 2.6). At a volume density of $\rho_0 \sim \epsilon^{-2}(H_x/H_B)\rho_{sx} \sim 7 \times 10^{-8}(H_x/H_B)$ g cm^{-3}, the Saha equations for sodium and potassium give an ion number density $n_i^{(0)} \sim 1 \times 10^4 (H_x/H_B)^{1/2}$ cm^{-3} for $T_x =$ 1000 K, and $n_i^{(0)} \sim 6 \times 10^7 (H_x/H_B)^{1/2}$ cm^{-3} for $T_x = 1500$ K. The high sensitivity of the ion density to T_x implies that slight adjustments of R_x in a CTTS disk, presumably through the dependence of α_x on the dimensionless parameter $\Omega_x t_{ni}^{(0)}$, can yield a location for the X-point that corresponds to almost any desired rate of magnetic diffusion.

As an example, if we adopt the central electron and ion number densities, $n_e^{(0)} = n_i^{(0)} \sim 10^5 (H_x/H_B)^{1/2}$ cm^{-3}, then $\rho_i^{(0)} \sim 5 \times 10^{-18}(H_x/H_B)^{1/2}$ g cm^{-3} for $m_i \sim 30 m_H$. Substitution of the latter value into equations (3.2a)–(3.2b) yields $v_d^{(0)}/a_x \sim 0.07(H_B/H_x)^{1/2}$; i.e., neutrals drift modestly with respect to the field in the midplane. Averaged over the thickness of the disk, $\bar{v}_d \sim \dot{M}_D/2\pi R_x \sigma_x \sim (\dot{M}_D/\dot{M}_w)\epsilon^2 a_x \sim 2 \times 10^{-3} a_x$ (see eqs. [2.11c] and [3.3b]).

Additional processes enter to complicate the simple situation described above. Near the midplane, the gyrofrequency of an ion (Na^+ or K^+), $\omega_{Bi} = eB/m_i c$, is small compared to the collision frequency of the same ion in a sea of neutrals, $t_{in}^{-1} = \gamma_{in}\rho$; i.e., $\omega_{Bi}^{(0)}/\gamma_{in}\rho_0 \sim 0.03(H_B/H_x)^{1/2}$ for the numbers used above. Ions at the midplane are therefore not well tied to field lines and may be dragged across them by collisions with neutrals at a velocity equal to a significant fraction of a_x.

To supply the current needed for the given curl of $\boldsymbol{B}$, the drift velocity of ions with respect to electrons (mostly in the φ-direction) $\boldsymbol{v}_{ie} = (c/4\pi n_e e)(\nabla \times \boldsymbol{B})$. Applied to the midplane of the wind portion of the X-region, the required ion-electron drift speed $v_{ie}^{(0)} \sim cB_x/4\pi n_e^{(0)} e H_B \sim 4 \times 10^5 (H_x/H_B)^{1/2}$ cm s^{-1}, which is comparable to the rotational excesses and deficits of midplane ions relative to field lines (for $a_x \sim 2 \times 10^5$ cm s^{-1}).

With gyrofrequencies larger than those of ions by a factor m_i/m_e, electrons would seem better tied to field lines. But collisions with neutrals are still efficient at knocking electrons off field lines and thereby contributing to the ohmic dissipation. If we assume that ions and neutrals at the midplane nearly move together, the electrical resistivity of the disk plasma is given by (cf. eq. [21.18] of Shu 1992):

$$\eta_D = \frac{c^2 \nu_{en}}{\omega_{pe}^2}, \tag{3.5}$$

where $\omega_{pe}^2 = 4\pi n_e e^2/m_e$ is the square of the electron plasma frequency and $\nu_{en} \equiv \gamma_{en}\rho$ is the collision frequency of an electron in a sea of neutrals. From equations (13) and (14) of Draine, Roberge, & Dalgarno (1983), we get $\gamma_{en} \approx 7 \times 10^{15}$ cm^3 g^{-1} s^{-1} for $T_x = 1100$ K, and $\eta_D^{(0)} \sim 1 \times 10^{15}(H_x/H_B)^{1/2}$ cm^2 s^{-1}. The diffusion time for electrons across field lines in the midplane $\sim H_B^2/\eta_D^{(0)} \sim 3 \times 10^5 (H_B/H_x)^{5/2}$ s, which is crudely comparable to Ω_x^{-1} if $H_B \sim H_x$. Equation (13.4.2) of Umebayashi & Nakano (1988) also implies that ohmic dissipation and ambipolar diffusion are roughly competitive if

[2] This effect, added to the hole in the inner disk, may lead to insufficient near-infrared excess in comparison with standard disk/star models of CTTSs (Hartmann 1993, personal communication). However, if the X-wind levitates dust from the disk, then the reprocessing of starlight by this dust may refill the deficit of near-infrared radiation.

$B_x \sim 2 \times 10^2$ G, $n_H \sim 10^{16}$ cm^{-3}, and $H_B \sim H_x$. Integrated over the thickness of the disk, the heat released per unit area by ohmic dissipation then probably has the same order of magnitude as the expression (3.4).

In summary, field freezing to the *neutrals* constitutes a good approximation everywhere in the X-region of a CTTS except near the midplane. At the midplane, the more general formulae of Nakano & Umebayashi (1988; see their eqs. [6.3.2]–[6.3.4]) confirm our conclusion that neutrals have appreciable slip velocities perpendicular to $\boldsymbol{B}$, both parallel to the Lorentz force per unit volume $[(\nabla \times \boldsymbol{B}) \times \boldsymbol{B}]/4\pi$ (i.e., in the ϖ direction) and perpendicular to it (i.e., in the φ direction). A deep physical connection may exist therefore between the numerical coincidences noted for T Tauri stars (1) in § 2.1 between the corotation radius and the distance for marginal coupling to embedded magnetic fields, and (2) in § 2.7 for R_x to occur close to the crossover radius where accretional heating begins to affect reprocessing heating (cf. eq. [2.8]).

3.2. *Macroscopic Mechanisms*

Stable self-regulation may also occur by a more speculative route. If too high an ionization level presents a bottleneck to the loading of field lines for the X-wind flow, the midplane density may rise relative to the sonic density above the value given by equation (2.10b). The onset of multiple-fluid forms of the Balbus-Hawley instability may then provide an effective "turbulent" diffusivity that helps with the loading of field lines at the proper rate, even in the X- and T-regions and not just the dead zone. This state of affairs may apply to the class of CTTSs with effective temperatures $T_* > 4500$ K, whose rotation periods peak at $\sim$4d (see Edwards et al. 1993b; see also the case of SU Aur discussed in § 5.2).

In other circumstances—e.g., binary X-ray sources—with high rather than order-unity "magnetic Reynolds numbers," the difficulty for gas to diffuse microscopically across field lines at anything approaching adequate rates (e.g., if $\Omega_x t_{ni}^{(0)} \ll 1$) may cause the central density greatly to exceed the value given by equation (2.10b). In these circumstances, even the most violent forms of the Balbus-Hawley instability may not suffice to load field lines fast enough for the wind and funnel flows to empty the X- and T-regions against the input by viscous accretion. In a highly conducting medium, the action of the Balbus-Hawley instability also tends to disconnect the fields interior and exterior to the disk. In these circumstances, corotation of the region between R_t and R_x with the star may not be maintained in steady state. The large shear rates between conducting disk fluid and excluded stellar magnetic field may now yield fully developed turbulence of the kind envisaged by Arons (1986, 1987), with consequences that may help to explain why X-ray pulsars commonly spin up during accretion while classical T Tauri stars do not.[3] With some inventiveness, one might even be able to come up with a plausible scenario that would give rise to two possible kinds of solutions for YSOs: a low (ionization and accretion) state represented by the CTTSs and a high state represented by the FU Orionis outburst sources (Hartmann et al. 1993).

[3] Recent discoveries by *Ginga* and BATSE of long-term spin evolution in two X-ray pulsars, GX 1 + 4 (Makishima et al. 1988; Chakrabarty et al. 1994) and 4U 1616−67 (Bildsten et al. 1994), that had previously been spinning up for $\gtrsim$10 yr, suggest that spin-down occurs nearly as commonly as spin-up in these systems.

4. GLOBAL PROPERTIES OF THE X-CELERATOR WIND

4.1. *Mass-Loss Rate*

In this section, we use conservation relations to derive certain global properties of the X-wind. We begin by finding, in steady state, the relationship between the mass-loss rate $\dot{M}_w$ in the X-wind and the accretion rate $\dot{M}_D$ flowing from the disk proper into the X-region. For this global purpose, we may regard the X-region as a single point at R_x from which a wind flow emerges, with a disk outside of this point and with a funnel flow somewhat inside it.

Consider the angular momentum balance for all the material interior to R_x. The star, the disk, the dead zone, and the funnel flow inside the stellar magnetopause have complicated magnetic interactions along closed field lines (whose detailed elucidation we leave for future work), but since these interactions (and any viscous ones) involve purely *internal torques*, they can only *redistribute* the angular momentum among the various connected components. Since the star represents the largest reservoir by far for the accreting material, the rate of change of the angular momentum of the system inside the magnetopause over any appreciable length of time essentially equals the time derivative of the stellar angular momentum $bM_* R_*^2 \Omega_*$, where b is a dimensionless measure of the star's moment of inertia. For a fully convective star, $b = 0.205$ if it spins slowly and $b = 0.136$ if it spins at breakup (James 1964).

Against the internal change, we must balance the external contributions. First, we have the inflow of angular momentum by disk accretion $\dot{M}_D R_x^2 \Omega_x$. Second, we have the viscous torque exerted by material outside R_x on material inside R_x (see eq. [7.13] of Shu 1992):

$$\mathcal{T}_x = \left(2\pi\varpi^2 \nu_D \sigma \frac{d\Omega}{d\varpi}\right)_x , \tag{4.1}$$

where the subscript "x" denotes that all quantities are to be evaluated at R_x. In terms of our previous notation, $\Omega = \Omega_x + \langle u_\varphi \rangle/\varpi$, with $\langle u_\varphi \rangle$ being an appropriately averaged value over the vertical thickness of the disk. The viscous torque T_x is negative if $d\Omega/d\varpi < 0$ at the X-point. If the disk is effectively nonconducting beyond R_x, the origin of this viscous torque must lie in a nonmagnetic mechanism, such as turbulent convection (see, e.g., Adams & Lin 1993).

Third, we have a net removal of angular momentum from the X-region by the wind, $\dot{M}_w \bar{J} R_x^2 \Omega_x$, where the dimensionless quantity $\bar{J}$ is defined as the total specific angular momentum $j(\psi)$ carried in the wind (see eq. [2.7]), averaged over all streamlines (see eq. [4.13b]), and measured in units of $R_x^2 \Omega_x$. Angular momentum conservation requires that the time rate of change of the internal amount equals the external inputs and torques

$$\frac{d}{dt}(bM_* R_*^2 \Omega_*) = (1 - \tau)\dot{M}_D R_x^2 \Omega_x - \dot{M}_w \bar{J} R_x^2 \Omega_x , \tag{4.2a}$$

where we have defined the (positive) dimensionless ratio,

$$\tau \equiv -\frac{\mathcal{T}_x}{\dot{M}_D R_x^2 \Omega_x} . \tag{4.2b}$$

Mass conservation requires

$$\dot{M}_* = \dot{M}_D - \dot{M}_w . \tag{4.3}$$

In setting up the balances of equations (4.2a) and (4.3), we have for simplicity ignored any contribution from an ordinary stellar wind.

Equation (4.2a) can be derived more formally by integrating the angular momentum equation

$$\frac{\partial}{\partial t}(\rho j_g) + \nabla \cdot \left[(j_g + j_B)\rho \boldsymbol{u} + \rho \varpi^2 \nu_D \frac{d\Omega}{d\varpi} \boldsymbol{e}_\varpi \right] = 0$$

over a large cylindrical volume that extends just beyond R_x. (See § 2.6 for the definitions of j_g and j_B.) Thus, the term on the left-hand side of equation (4.2a) represents a volume integral of the first term above; the term $-\dot{M}_w \bar{J} R_x^2 \Omega_x$ represents the wind contribution when we transform the divergence term to a surface integral above and below the disk; and the term proportional to $(1 - \tau)$ represents the contribution from the same divergence term due to the part of the cylindrical surface that lies within the disk. The quantity τ is then effectively evaluated as a vertical integral over a thin disk at the outer boundary of the X-region, R_x^+.

In the formula $R_x = \Gamma_x R_*$, the coefficient Γ_x does not depend very sensitively on the stellar and disk parameters of the problem, if we assume α_x is a constant in equation (2.6b). To avoid having to discuss the time-dependence of B_* (via the response of the stellar dynamo to a changing M_* and Ω_*), we adopt the simplifying ad hoc assumption that Γ_x equals a constant independent of time.

We also assume that low-mass stars quasi-steadily accreting and burning deuterium increase their radii at a rate proportional to their fractional increase of mass (e.g., Palla & Stahler 1991):

$$\frac{\dot{R}_*}{R_*} = \frac{\dot{M}_*}{M_*} . \tag{4.4}$$

Taking the logarithmic derivatives in time of equations (2.3a) and (2.6a), together with the substitution $\Omega_* = \Omega_x$, now yields

$$\frac{\dot{\Omega}_*}{\Omega_*} = -\frac{\dot{M}_*}{M_*} . \tag{4.5}$$

With b assumed a constant, equation (4.2a) becomes

$$2b\dot{M}_* = (1 - \tau)\Gamma_x^2 \dot{M}_D - \Gamma_x^2 \bar{J} \dot{M}_w , \tag{4.6}$$

which with the substitution of equation (4.3) can be solved to obtain equation (1.1) with

$$f = \frac{1 - \tau - 2b_{\rm eff}}{\bar{J} - 2b_{\rm eff}} , \tag{4.7a}$$

where

$$b_{\rm eff} \equiv b/\Gamma_x^2 . \tag{4.7b}$$

If $\Gamma_x = 5.7$ typically, $2b_{\rm eff}$ is a very small number ($\lesssim 0.02$) and can generally be ignored in both the numerator and denominator of equation (4.7a). In this case, many of the assumed detailed properties of the star used to derive equation (4.7a) have no practical consequences, once we scale the problem to reflect the conditions at the X-point (see Papers II and III).

Equations (1.1) and (4.7a)–(4.7b) recover the result stated by SLRN if we ignore any viscous torque and place the X-point at the stellar radius, i.e., set $\tau = 0$ and $\Gamma_x = 1$ so that $b_{\rm eff} = b$ and the star rotates at breakup. In the more general case when $0 < \tau < (1 - 2b_{\rm eff})$ and $\Gamma_x > 1$, the X-wind and the magnetic stresses internal to the disk ultimately provide whatever braking torque is not supplied by the viscous torque so that the eventual specific angular momentum of the accreting material does not spin up the star beyond corotation with the X-region.

Without detailed knowledge of the disk viscosity and a calculation of the flow in the X-region and dead zone, we cannot assign a precise value to τ. For ϖ somewhat greater than R_x (i.e., outside the X-region), the viscous torque $|\mathcal{T}|$ (due, e.g., to turbulent convection) has no competition and suffices to remove angular momentum from the interior at a rate approximately equal to $\dot{M}_D R_x^2 \Omega_x$. If we assume that the kinematic viscosity ν_D remains about the same in the X-region, the viscous torque $|\mathcal{T}_x|$ is (much) smaller than $\dot{M}_w R_x^2 \Omega_x$ according to equation (4.1), since the surface density σ and angular shear rate $d\Omega/d\varpi$ are (much) smaller at R_x than just beyond R_x (see § 2.7). This scaling argument would seem to suggest that $\tau \ll 1$ in equation (4.2b) and can therefore effectively be ignored in equation (4.7a), an argument similar in form to that given by Lynden-Bell & Pringle (1974) for viscous boundary layers abutting a slowly rotating star where $d\Omega/d\varpi$ is also envisaged to go through a zero. Unfortunately, the disk "viscosity" in the dead zone (and perhaps even the X- and T-regions) is more likely to be due to the Balbus-Hawley-Wardle-Königl mechanism than to convective turbulence; thus, we cannot justify the assumption that ν_D maintains the same value in these magnetized regions as it does in the non-magnetized regions. Nevertheless, we find it difficult to imagine that, on field lines which have a favorable open geometry, the Balbus-Hawley-Wardle-Königl part of the magnetocentrifugal mechanism could be much more efficient than the X-wind part of the mechanism. Hence, we anticipate that detailed calculations of the complex interactions will show that $\tau \lesssim \frac{1}{2}$, and perhaps $\ll 1$.

In Papers II and III we shall compute *maximum* values of f by assuming that $\tau = 0$. This assumption does not imply, however, that we believe the angular momentum carried away in the wind comes entirely from the material at the base of the wind (the X-region). On the contrary, we hold that the wind arises basically because the accreting star has an angular momentum problem that its magnetosphere transfers to the disk (via magnetic funnel flow). This "solution" creates a problem for the disk because it drastically lowers the local shear rate (and surface density) of the disk, thereby reducing the efficiency of viscous transport of mass in and angular momentum out. The rest of the "problem" is then solved (with or without angular momentum transport across a dead zone depending on the tilt of the stellar magnetosphere) by the disk blowing an induced wind.

How does the X-wind self-regulate dynamically as to carry away just the amount of angular momentum that viscous transport does not? Suppose the X-wind blows at a rate less than the equilibrium value given by equation (1.1). Then viscous transport from the disk brings to the X-region more matter than is removed in steady state. The density at the sonic surface would rise, the X-point field would be pinched to greater strengths, and the X-wind would gain in power until $\dot{M}_w$ did equal the equilibrium value. A similar argument for the opposite case shows that $\dot{M}_w$ would fall to the equilibrium value if initially it exceeded $f\dot{M}_D$.

If the disk totally excludes the stellar field (i.e., if the disk resistivity were zero), viscous accretion without any competition would make $\tau = 1 - 2b_{\rm eff}$, and would ultimately force the disk to extend at Keplerian speeds right down to the surface of the central star. In such a situation, the viscous torques imparted to the star would sooner or later spin it to breakup (see, e.g., Paczyński 1991; Popham & Narayan 1991), and the star would develop an X-wind of the type depicted in Figure 1. In all circumstances, therefore, we believe the initi-

ation of an X-celerator flow to be almost inevitable if the central object is sufficiently magnetized.

4.2. *Terminal Velocity*

In this section we estimate the terminal velocity of the X-wind. In a frame that corotates with the X-point, if we ignore terms of relative order ϵ^2, Bernoulli's theorem reads (see Paper II)

$$\tfrac{1}{2}|\boldsymbol{u}|^2 + V_{\rm eff} = 0\,, \tag{4.8}$$

where $V_{\rm eff}$ is the effective potential given by equation (2.3b). Equation (4.8) implies that the fluid velocity $\boldsymbol{u}$ measured in a frame that rotates at angular speed Ω_x goes to zero as we approach the X-point. More precisely, if we retain the accurate form of the Bernoulli equation, $|\boldsymbol{u}| \to a_x = \epsilon R_x \Omega_x$ when we are within order ϵR_x of the X-point.

At large distances from the X-point, equation (4.8) takes the approximate form,

$$\tfrac{1}{2}|\boldsymbol{u}|^2 - \tfrac{1}{2}\Omega_x^2 \varpi^2 + \tfrac{3}{2}\Omega_x^2 R_x^2 = 0\,. \tag{4.9}$$

We keep the last term in equation (4.9), which is only order unity, because the first two terms on the right-hand side, while individually large, have opposite signs and nearly cancel since the apparent fluid velocity $\boldsymbol{u}$ almost entirely reflects frame rotation at large ϖ. More meaningful than $\boldsymbol{u}$ in these circumstances is the velocity in an inertial frame,

$$\boldsymbol{v} \equiv \boldsymbol{u} + \Omega_x \varpi \boldsymbol{e}_\varphi\,. \tag{4.10}$$

Rearranging terms and squaring, we obtain

$$|\boldsymbol{u}|^2 = |\boldsymbol{v}|^2 + \Omega_x^2 \varpi^2 - 2J_g R_x^2 \Omega_x^2\,, \tag{4.11}$$

where $J_g \equiv j_g/R_x^2\Omega_x$ is the dimensionless version of the specific angular momentum of the gas, $j_g = \varpi v_\varphi$, introduced in § 2.6. Since J_g is a number of order unity, $v_\varphi \to 0$ as $\varpi \to \infty$, and we may write $|\boldsymbol{v}| \to (v_\varpi^2 + v_z^2)^{1/2} \equiv v_w$ for the terminal velocity of the wind. Substituting equation (4.11) into equation (4.9) and taking the limit $\varpi \to \infty$, we obtain

$$v_w = (2J_g - 3)^{1/2} R_x \Omega_x\,. \tag{4.12}$$

Since $J_g \le J(\psi) = J_g + J_B$, where J_g and J_B are both positive for the X-wind (cf. §§ 2.5 and 2.6), the root-mean-square terminal velocity satisfies the result quoted in SLRN,

$$\bar{v}_w \le (2\bar{J} - 3)^{1/2} R_x \Omega_x\,, \tag{4.13a}$$

where

$$\bar{J} \equiv \int_0^1 J(\psi) d\psi \tag{4.13b}$$

is the average of $J(\psi)$ over all streamlines (in either hemisphere) labeled from $\psi = 0$ to $\psi = 1$ (see Papers II and III).

4.3. *Total Energy Carried in the Wind*

The wind luminosity $L_w = L_g + L_B$ is composed of two parts, a part carried in the gas,

$$L_g = \tfrac{1}{2}\dot{M}_w \bar{v}_w^2 = (\bar{J}_g - \tfrac{3}{2})\dot{M}_w R_x^2 \Omega_x^2\,, \tag{4.14a}$$

and a part carried in the field,

$$L_B = \int \frac{c}{4\pi}(\boldsymbol{E} \times \boldsymbol{B}) \cdot \hat{\boldsymbol{n}}\, dA\,, \tag{4.14b}$$

where $c(\boldsymbol{E} \times \boldsymbol{B})/4\pi$ is the Poynting flux measured in an inertial frame, and $\hat{\boldsymbol{n}}$ is the unit normal of an element of area dA oriented perpendicularly to the Poynting flux. A little thought suffices to show that, as $\varpi \to \infty$, $\hat{\boldsymbol{n}}$ lies in the meridional plane and is parallel to the poloidal component of the fluid velocity. If we adopt the assumptions of ideal MHD, where the magnetic field $\boldsymbol{B} = \beta\rho\boldsymbol{u} \to \beta\rho u_\varphi \boldsymbol{e}_\varphi$ and the electric field (cf. eq. [21.30] of Shu 1992)

$$\boldsymbol{E} = -\frac{\boldsymbol{v}}{c} \times \boldsymbol{B} \to -\frac{v_w}{c}\beta\rho u_\varphi(\hat{\boldsymbol{n}} \times \boldsymbol{e}_\varphi) \to \frac{v_w}{c}\beta\rho\varpi\Omega_x(\hat{\boldsymbol{n}} \times \boldsymbol{e}_\varphi)\,, \tag{4.15}$$

we obtain

$$\frac{c}{4\pi}(\boldsymbol{E} \times \boldsymbol{B}) \to J_B R_x^2 \Omega_x^2 \rho v_w \hat{\boldsymbol{n}}\,, \tag{4.16}$$

where we have used a result from § 2.6 to identify $-\varpi\beta^2\rho u_\varphi/4\pi$ as $J_B R_x^2 \Omega_x$. The substitution of equation (4.16) into equation (4.14b) yields

$$L_B = \bar{J}_B \dot{M}_w R_x^2 \Omega_x^2\,, \tag{4.17a}$$

where $\bar{J}_B$ is the streamline-averaged value of J_B in the X-wind and we have identified

$$\dot{M}_w = \int (\rho v_w \hat{\boldsymbol{n}}) \cdot \hat{\boldsymbol{n}}\, dA\,, \tag{4.17b}$$

as the mass-loss rate. If we sum equations (4.14a) and (4.17a), we get for the total wind luminosity,

$$L_w = (\bar{J} - 3/2)\dot{M}_w R_x^2 \Omega_x^2\,. \tag{4.18}$$

Using equations (1.1) and (2.3a), with the approximation $f \approx (1 - \tau)/\bar{J}$ (cf. the discussion after eq. [4.7a]), we may rewrite equation (4.18) in the suggestive approximate form,

$$L_w \approx (1 - \tau)\left(1 - \frac{3}{2\bar{J}}\right)\frac{GM_* \dot{M}_D}{R_x}\,. \tag{4.19}$$

Equation (4.19) implies that the basic energy for driving the outflow comes from the release of gravitational energy in disk accretion at a rate $\dot{M}_D$. The part of the energy so released that does not go eventually into viscous dissipation compresses the stellar field at R_x. The compressed field B_x combines magnetocentrifugally with the stellar and disk rotation to launch an X-wind; i.e., we envisage the wind energy as ultimately extracted at the expense of a reduction of the rotational energy of the star and the inner part of the disk. (From the estimates of § 3.1, we see that only a minor fraction $\sim\epsilon^2$ of the mechanical energy of the process gets converted locally into heat at the X-region.) If viscous transport were negligible at the outer boundary of the X-region ($\tau \to 0$) and the field B_x could be compressed infinitely ($\bar{J} \to \infty$), equation (4.19) predicts that the total gravitational energy released per gram, GM_*/R_x, in moving matter from infinity to R_x could be used to drive a wind. In practice, we allow for a greater role for viscous torques (corresponding, say, to as much as $\tau \approx 0.5$) and a more modest compression of the field (corresponding, say, to $\bar{J} \approx 3$), so that fractions like one-fourth of this value might be more typical.

5. DISCUSSION

5.1. *Summary of Theory*

Many independent lines of theoretical investigation on the interaction of stellar magnetic fields and accretion disks have converged in this paper. Application of the resulting theory to T Tauri stars and low-mass protostars lead us to conclude:

1. Stellar magnetic fields strong enough to truncate a conducting disk with mass accretion rate $\dot{M}_D$ (Königl 1991) also automatically have sufficient strength to drive a magneto-centrifugal wind with mass-loss rate $\dot{M}_w$ not much smaller than $\dot{M}_D$. In particular, for an aligned stellar magnetosphere, the natural corotation radius R_x (where the disk has a Keplerian angular velocity Ω_x that matches the angular velocity Ω_* of the star) has a value (eqs. [2.6a]–[2.6b]) that resembles the formula (eqs. [2.2a]–[2.2b]) for the disk truncation radius R_t from the theory of Ghosh & Lamb (1978, 1979a, b). Exterior to R_t (T-region) and to R_x (X-region), respectively, funnel and wind flows emerge. Figure 4 illustrates the situation on a large scale; Figure 3, on a small scale.

2. The X-region has a fractional size roughly equal to ϵ, the ratio of the local isothermal speed of sound a_x to the orbital speed $R_x\Omega_x$. The distance of the T-region from the X-region depends on (currently unknown) details of the field geometry: R_t could be as small a 0.72 R_x if the stellar dipole has no tilt with respect the disk rotation axis and angular momentum transport across the dead zone is efficient; alternatively, R_t could essentially equal R_x if this tilt is substantial ($\gtrsim 30°$), or if dead-zone torques are inefficient and fields pinch toward the X-point. In the last case, the fractional size of the T-region is probably also roughly equal to ϵ. Both the T- and X-regions rotate at nearly the same angular velocity $\Omega_* = \Omega_x$.[4] The ability of the magnetic fields to enforce this condition may depend, however, on the magnetic diffusivity in the disk being fairly large (e.g., a lightly ionized disk).

3. For parameters appropriate to most CTTSs, loading of accreting disk matter at steadystate rates onto the field lines involved in the wind and funnel flows can occur by the ordinary microscopic mechanisms of ambipolar diffusion and ohmic dissipation. Because these flows originate from two nearby regions, slight adjustments of R_x about the position of marginal electromagnetic coupling in the midplane of the disk can probably yield the requisite microscopic rates. If R_x is initially too far from the star, matter loads diffusively onto closed field lines at a faster-than-equilibrium rate, and the corresponding spinup of the system interior to R_x will move the corotation radius inward. If R_x is initially too close to the star, inwardly diffusing matter which first encounters open field lines loads preferentially onto these field lines rather than onto closed field lines. The resulting spin-down of the system interior to R_x by the X-wind will move R_x outward. In hotter sources, the microscopic mechanisms may fail, and macroscopic instabilities, such as those investigated by Balbus & Hawley (1991, 1992), may play a more important role in determining the ratio $\beta(\psi)$ of the magnetic field to mass flux on any given streamline labeled by ψ.

4. For the large mass accretion rates applicable (perhaps) to protostars and FU Orionis outbursts, equations (2.6a)–(2.6b), with α_x of order unity, predict that R_x will be forced onto the surface of the star. The outer layers of the star will then be spun to breakup, and an X-celerator wind will be driven in a manner identical to that proposed originally by SLRN.

5. In more realistic situations, the star may possess intrinsically open field lines along which an O-wind blows; SLRN proposed that the collimation of the O-wind by the X-wind gives rise to optical jets (see also Kwan & Tademaru 1988; Solf & Bohm 1993). The present set of authors take a more electric view and defer to observational judgment whether optical jets might not arise also from the interaction of the X-wind with the ambient gas.

6. Funnel flow from the T-region occurs onto the star, producing magnetic "hot spots" and an "ultraviolet excess" when the gas impacts the stellar surface. The inflow may occur without spinning up the star, i.e., with a transfer of angular momentum to the *disk*. This (surprising) conclusion depends on the ability of the strong magnetic field to enforce near-corotation with the star throughout the T-region.[5]

7. Only a fraction τ of the excess angular momentum transferred to the X-region can be removed by viscous torques as part of the general process of inward transport of mass and outward transport of angular momentum. The remaining fraction is carried off by a magnetocentrifugally driven X-wind induced by the disk accretion and the stellar field. The ratio f of $\dot{M}_w$ to $\dot{M}_D$ is given by equation (4.7a), where the term $2b_{\rm eff}$ can be ignored to a first approximation, and where $\bar{J}$ is the dimensionless specific angular momentum carried off as an average by the streamlines of the X-wind. Paper III supplies, among other information, tabulations of the number $\bar{J}$ for different assumptions of the resultant magnetic field strengths (and loading of matter on field lines) at the base of the X-wind.

5.2. *Application to the T Tauri Star SU Aurigae*

Misaligned stellar magnetospheres and higher multipole moments (e.g., large magnetic loops) offer attractive variations of our picture to explain the night-to-night fluctuations of the emission-line profiles often associated with T Tauri stars. In particular, the extended set of observations of SU Aur by Johns et al. (1992; see also Giampapa et al. 1993) may already offer support for our theory. On analyzing the time-series properties of the blueshifted absorption component of the Hα line (at -150 km s^{-1} and identified as a wind component in the system), these authors find a clear signature at the rotation period of the star ($2\pi/\Omega_* = 3^{\rm d}$; see Herbst et al. 1987). If this wind arises in a disk, then its source corotates with the star; i.e., the wind originates from the X-region. For $M_* = 2.25\ M_\odot$ and $R_* = 3.6\ R_\odot$ (Bertout et al. 1988), $2\pi/\Omega_x = 3^{\rm d}$, for $R_x = 11\ R_\odot$, which implies $\Gamma_x = 3$. A factor $\Gamma_x = 3$, with $\alpha_x = 1$ in equation (2.6b) and $\dot{M}_D = 6 \times 10^{-8}\ M_\odot\ {\rm yr}^{-1}$ (Bertout et al. 1988), would require $B_* = 300$ G. This equatorial field strength is lower by a factor of 3 than the surface-averaged value (1000 G) measured for the weak-lined T Tauri star TAP 35 by Basri, Marcy, & Valenti (1992), but then SU Aur is of considerably earlier spectral type (G2) than TAP 35 (K1).

Extrapolating a stellar value, $B_* = 300$ G, as a dipole field yields $B_*(R_*/R_x)^3 = 11$ G, if $\Gamma_x = 3$. At a distance $s = 0.05R_x$ from the X-point (the nominal "patching" point for the X-wind calcultions of Paper III), the pinched X-region field will be about a factor $(0.05)^{-1} = 20$ larger, or $B_{\rm in} = 220$ G. (This extrapolation comes from taking the "inner limit of the outer solution" and only serves as reference value to scale the X-wind solution. The actual field B_x in the X-region may differ from the reference value $B_{\rm in}$ by factors of order unity without affecting this part of our scaling. See Paper III for a more accurate and extended discussion.) We nondimensionalize the

[4] Slight departures from strict uniform rotation may slowly twist up initially closed field lines and account for the large radio and optical flares known to take place on CTTSs.

[5] Without a more detailed theory of the disk and corona structure, we do not know how to estimate the amount of spin-up torque exerted on the star by the disk via the corona in the dead zone. It is conceivable that in some situations, this spin-up tendency outweighs the spin-down effect of the funnel flow.

reference value B_{in} by the fiducial field strength $B_{fid} \equiv (\Omega_x \dot{M}_w/R_x)^{1/2}$ that we use as the unit of field strength in our calculations of Papers II and III. For the set of parameters given above, $B_{fid} = 6.3$ G if the wind mass-loss rate $\dot{M}_w = 2 \times 10^{-8}\ M_\odot\ \mathrm{yr}^{-1}$, as is roughly required for self-consistency (see below; Kuhi [1966] cites $\dot{M}_w = 2.5 \times 10^{-8}\ M_\odot\ \mathrm{yr}^{-1}$).

Thus, $B_{in}/B_{fid} = 35$. Examining the columns of dimensionless B_{in} at the nondimensional reference position $q = 0.05$ in Table 4 of Paper III, we find that B_{in} is 31 (close enough to 35) in models 3 and 4 when the Alfvén surface lies at a nondimensional equatorial distance $q_A = 1$ from the X-point (i.e., when $\varpi_A \approx 2R_x = 6$). For these models, $\bar{J} \approx 3.5$, so the theoretical equilibrium ratio $\dot{M}_w/\dot{M}_D = f \approx \bar{J}^{-1}$ (cf. eq. [4.7a]), in rough agreement with the measured ratio. At the Alfvén surface, the mean poloidal fluid velocity ≈ 1.1 in units of $R_x\Omega_x = \Gamma_x\Omega_* R_* = 190$ km s^{-1}, or ~ 210 km s^{-1} in our example. In this interpretation, the absorption feature at -150 km s^{-1} in SU Aur would correspond to the region where the X-wind is still accelerating to full speed, perhaps accounting for the moderate line width of the feature (70 km s^{-1} FWHM). The mean terminal velocity of the wind $\bar{v}_w \lesssim (2\bar{J} - 3)^{1/2} R_x\Omega_x \approx 380$ km s^{-1} (cf. eq. [4.13a]), in rough agreement with the half-width at zero intensity of the "flat-topped" feature that Johns et al. (1992; see also Giampapa et al. 1993) ascribe to a fully developed wind.

While we would not want to attribute too much significance to these rough estimates, we do find it encouraging that even a preliminary analysis seems to give reasonable accord with the observations. We are particularly pleased by the following development which took place *after* it became clear that our theory predicts that inflow features connected with funnel flow from the *disk* should also show the periodicity of the *star*. An earlier analysis of redshifted hydrogen-line features in SU Aur had revealed no periodicity at all. A reanalysis based on a separate binning of the individual velocity channels reveals variability at the photometric period of the star (C. M. Johns 1994, personal communication), *and* a phase shift $\sim 180°$ with respect to the blueshifted feature (cf. § 2.3).

Stellar magnetic cycles and disk outbursts present similar opportunities for an inproved understanding of longer-term temporal variations indicated for many optical jets (Reipurth 1990; Raga & Kofman 1992). For a start on limiting the many possible variations on a common theme, we call for high resolution spectroscopic observations and modeling of YSOs (e.g., Welty et al. 1992; Calvet, Hartmann, & Kenyon 1993) to discriminate astronomically among the models in Figures 1, 2*a*, 2*b*, and 2*c*, or to eliminate them altogether.

We thank J. Arons, G. Basri, S. Edwards, A. Glassgold, C. Johns, and A. Königl for insightful discussions. We also thank the referee for this series of papers, L. Hartmann, for comments that clarified the arguments and presentation. This work was founded in part by NSF AST-9024260 and in part under the auspices of a special NASA Astrophysics Theory Program that supports a joint Center for Star Formation Studies at NASA/Ames Research Center, the University of California at Berkeley, and the University of California at Santa Cruz.

REFERENCES

Adams, F. C., Lada, C. J., & Shu, F. H. 1988, ApJ, 326, 865
Adams, F. C., & Lin, D. N. C. 1993, in Protostars and Planets III, ed. E. H. Levy & J. Lunine (Tucson: Univ. of Arizona Press), 721
Aly, J. J. 1980, A&A, 86, 192
André, Ph., Montmerle, T., Stine, P. C., Feigelson, E. D., & Klein, K. L. 1988, ApJ, 335, 940
André, Ph., Phillips, R. B., Lestrade, J. F., & Klein, K. L. ApJ, 376, 630
Arons, J. 1986, in Plasma Penetration into Magnetospheres, ed. N. Kylafis, J. Papamastorakis, & J. Ventura (Iraklion: Crete Univ. Press), 115
———. 1987, in IAU Symp. No. 125, The Origin and Evolution of Neutron Stars, ed. D. J. Helfand & J.-H. Huang (Dordrecht: Reidel), 207
———. 1993, ApJ, 408, 160
Attridge, J., & Herbst, W. 1992, ApJ, 398, L61
———. 1994, in preparation
Bachiller, R., & Cernicharo, J. 1990, A&A, 239, 276
Balbus, S. A., & Hawley, J. F. 1991, ApJ, 376, 214
———. 1992, ApJ, 400, 595
Bally, J., & Stark, A. A. 1983, ApJ, 266, L61
Basri, G., Marcy, G. W., & Valenti, J. A. 1992, ApJ, 390, 622
Beckwith, S., Sargent, A. I., Chini, R., & Gusten, R. 1990, AJ, 99, 924
Bertout, C. 1987, in Circumstellar Matter, ed. I. Appenzeller & C. Jorden (Dordrecht: Reidel), 23
———. 1989, ARA&A, 27, 351
Bertout, C., Basri, G., & Bouvier, J. 1988, ApJ, 330, 350
Bildsten, L., Chakrabarty, D., Chiu, J., Finger, M., Grunsfeld, J., Koh, T., Prince, T., & Wilson, R. 1994, in Proc. 2d Compton Gamma-Ray Symp., in press
Blandford, R. D., & Payne, D. G. 1982, MNRAS, 199, 883
Bouvier, J. 1990, AJ, 99, 946
Bouvier, J., Cabrit, S., Fernandez, M., Martin, E. L., & Matthews, J. M. 1993, A&A, 272, 176
Cabrit, S., Edwards, S., Strom, S. E., & Strom, K. M. 1990, ApJ, 354, 687
Calvet, N., Hartmann, L., & Kenyon, S. J. 1993, ApJ, 402, 623
Calvet, N., Patino, A., Magris, G., & D'Alessio, P. 1991, ApJ, 380, 617
Camenzind, M. 1990, in Reviews in Modern Astronomy 3, ed. G. Klare (Berlin: Springer), 259
Carlstrom, J., et al. 1994, in preparation
Chakrabarty, D., Bildsten, L., Chiu, J., Grunsfeld, J., Kohl, T., & Prince, T. 1994, in Proc. 2d Compton Gamma-Ray Symp., in press
DeCampli, W. M. 1981, ApJ, 224, 124
Draine, B. T. 1983, ApJ, 270, 519
Draine, B. T., Roberge, W. G., & Dalgarno, A. 1983, ApJ, 264, 485
Edwards, S., Ray, T., & Mundt, R. 1993a, in Protostars and Planets III, ed. E. H. Levy & J. Lunine (Tucson: Univ. of Arizona Press), 567
Edwards, S., et al. 1993b, AJ, 106, 372
Feigelson, E. D., Casanova, S., Montmerle, T., & Guibert, J. 1993, ApJ, 416, 623
Fukui, Y. 1989, in Proc. ESO Workshop on Low-Mass Star Formation and Pre–Main-Sequence Objects, ed. B. Reipurth (Garching: ESO), 365
Galli, D. 1990, Ph.D. thesis, Univ. of Florence
Ghosh, P., & Lamb, F. K. 1978, ApJ, 223, L83
———. 1979a, ApJ, 232, 259
———. 1979b, ApJ, 234, 296
Giampapa, M. S., Basri, G. S., Johns, C. M., & Imhoff, C. L. 1993, ApJS, 89, 321
Giovanardi, C., Lizano, S., Natta, A., Evans, N. J., II, & Heiles, C. 1992, ApJ, 397, 214
Glassgold, A. E., Mamon, G. A., & Huggins, P. J. 1989, ApJ, 336, L29
———. 1991, ApJ, 373, 254
Hartmann, L., Kenyon, S., & Hartigan, P. 1993, in Protostars and Planets III, ed. E. H. Levy & J. Lunine (Tucson: Univ. of Arizona Press), 497
Hartmann, L., & MacGregor, K. B. 1982, ApJ, 259 180 (HM)
Hartmann, L., & Stauffer, J. R. 1989, AJ, 97, 873
Hawley, J. F., & Balbus, S. A. 1991, ApJ, 376, 223
———. 1992, ApJ, 400, 595
Hayashi, C., Nakazawa, K., & Nakagawa, Y. 1985, in Protostars and Planets II, ed. D. C. Black & M. S. Matthews (Tucson: Univ. of Arizona Press), 1100
Herbig, G. 1977, ApJ, 217, 693
Herbst, W., et al. 1987, AJ, 94, 137
Holzer, T. E., Flå, T., & Leer, E. 1983, ApJ, 275, 808
James, R. A. 1964, ApJ, 140, 552
Johns, C. M., Basri, G. S., Giampapa, M. S., & DeFonso, E. 1992, in Cool Stars, Stellar Systems, and the Sun, ed. M. S. Giampapa & J. A. Bookbinder (San Francisco: ASP), 441
Kenyon, S. J., & Hartmann, L. 1987, ApJ, 323, 714
Königl, A. 1989, ApJ, 342, 208
———. 1991, ApJ, 370, L39
Königl, A., & Ruden, S. P. 1993, in Protostars and Planets III, ed. E. H. Levy & J. Lunine (Tucson: Univ. of Arizona Press), 641
Koo, B.-C. 1989, ApJ, 337, 318
Kuhi, L. V. 1966, ApJ, 143, 991
Kwan, J., & Tademaru, E. 1988, ApJ, 332, L41
Lada, C. J. 1985, ARA&A, 23, 267
Lago, M. T. V. T. 1984, MNRAS, 210, 323
Lizano, S., Heiles, C., Rodriguez, L. F., Koo, B.-C., Shu, F. H., Hasegawa, T., Hayashi, S., & Mirabel, I. F. 1988, ApJ, 328, 763
Lovelace, R. V. E. 1976, Nature, 262, 649
Lynden-Bell, D., & Pringle, J. E. 1974, MNRAS, 168, 603
Makishima, K., et al. 1988, Nature, 333, 746
Masson, C. R., Mundy, L. G., & Keene, J. 1990, ApJ, 357, L25

Mestel, L. 1968, MNRAS, 138, 359
Montmerle, T., Feigelson, E. D., Bouvier, J., & André, Ph. 1993, in Protostars and Planets III, ed. E. H. Levy & J. Lunine (Tucson: Univ. of Arizona Press), 689
Mundt, R. 1985, in Protostars and Planets II, ed. D. C. Black & M. S. Matthews (Tucson: Univ. of Arizona Press), 414
Nakano, T., & Umebayashi, T. 1988, Prog. Theor. Phys., Suppl., 96, 73
Natta, A., & Giovanardi, C. 1990, ApJ, 356, 646
Natta, A., Giovanardi, C., & Palla, F. 1988, ApJ, 332, 921
Paczyński, B. 1991, ApJ, 370, 597
Palla, F., & Stahler, S. W. 1991, ApJ, 375, 288
Popham, R., & Narayan, R. 1991, ApJ, 370, 604
Pudritz, R. E., & Norman, C. A. 1983, ApJ, 274, 677
———. 1986, ApJ, 301, 571
Raga, A. C., & Kofman, L. 1992, ApJ, 386, 222
Reipurth, B. 1990, in Physics of Star Formation and Early Stellar Evolution, ed. C. J. Lada & N. D. Kylafis (Dordrecht: Kluwer), 497
Ruden, S. P., Glassgold, A. E., & Shu, F. H. 1990, ApJ, 361, 546 (RGS)
Ruiz, A., Alonso, J. L., & Mirabel, I. F. 1992, ApJ, 394, L57
Russell, A. P. G., Bally, J., Padman, R., & Hills, R. E. 1992, ApJ, 387, 219
Safier, P. N. 1993, ApJ, 408, 115
Scharleman, E. T. 1978, ApJ, 219, 617
Shu, F. H. 1992, The Physics of Astrophysics, Vol. 2 (Mill Valley, CA: University Science Books)
Shu, F. H., Lizano, S., Ruden, S. P., & Najita, J. 1988, ApJ, 328, L19 (SLRN)
Shu, F. H., & Terebey, S. 1984, in Cool Stars, Stellar Systems and the Sun, ed. S. Baliunas & L. Hartmann (Berlin: Springer), 78
Snell, R. L. 1987, in IAU Symp. 115, Star-forming Regions, ed. M. Peimbert & J. Jugaku (Dordrecht: Reidel), 213
Solf, J., & Bohm, K. H. 1993, ApJ, 410, L31
Stahler, S. W. 1983, ApJ, 274, 822
Strom, K. M., Strom, S. E., Edwards, S., Cabrit, S., & Skrutskie, M. F. 1989, AJ, 97, 1451
Uchida, Y., & Shibata, K. 1985, PASJ, 37, 515
Umebayashi, T., & Nakano, T. 1988, Prog. Theor. Phys., Suppl., 96, 151
Vogel, S. N., & Kuhi, L. V. 1981, ApJ, 245, 960
Wardle, M., & Königl, A. 1993, ApJ, 410, 218
Weber, E. J., & Davis, L. 1967, ApJ, 148, 217
Weidenschilling, S. J., & Cuzzi, J. N. 1993, in Protostars and Planets III, ed. E. H. Levy & J. I. Lunine (Tucson: Univ. of Arizona Press), 1031
Welty, A. D., Strom, S. E., Edwards, S., Kenyon, S. J., & Hartmann, L. W. 1992, ApJ, 397, 260